

## Article

# Molecular Phylogeny, Taxonomy and Distribution Patterns of Trichomycterine Catfishes in the Middle Rio Grande Drainage, South-Eastern Brazil (Siluriformes: Trichomycteridae)

Wilson J. E. M. Costa <sup>1,\*</sup>, Valter M. Azevedo-Santos <sup>2</sup>, José Leonardo O. Mattos <sup>1</sup> and Axel M. Katz <sup>1</sup>

<sup>1</sup> Laboratory of Systematics and Evolution of Teleost Fishes, Institute of Biology, Federal University of Rio de Janeiro, Rio de Janeiro 21941-901, RJ, Brazil

<sup>2</sup> Programa de Pós-Graduação em Biodiversidade, Ecologia e Conservação, Universidade Federal do Tocantins (UFT), Porto Nacional 77001-090, TO, Brazil

\* Correspondence: wcosta@acd.ufrj.br

**Abstract:** The Rio Grande drainage plays a key role in supplying water and electricity to large urban centres, but some components of its rich ichthyofauna are still poorly known. Based on our field inventories in the middle section of the drainage, we recognised 10 trichomycterine endemic species, of which 6 species are new and described herein. A molecular analysis (2600 bp for 43 taxa) indicated that the species of both subgenera do not form monophyletic groups. One species of the subgenus *Cryptocambeva* is closely related to species from the inner Brazilian Plateau, whereas other species of this subgenus are closely related to species endemic to smaller coastal basins. The species of the subgenus *Paracambeva* belong to different lineages of a clade endemic to the Rio Grande drainage. These species are diagnosed by the characters of their external morphology and osteology. A key to species identification is provided. The species distribution patterns support delimitation of three areas of endemism, which may have a relevant role for proposals of conservation strategies: the Uberaba, the São João-Sapucaí, and the Tamborete areas. The last one, a small area confined between the Serra da Canastra and the Rio Grande at the Furnas dam, is particularly important for sheltering three endemic trichomycterines and two loricariid catfishes.

**Keywords:** comparative osteology; mountain biodiversity; Rio Paraná basin; species conservation

**Key Contribution:** This study provides new accounts on mountain catfishes in a region combining high species diversity and environmental degradation; a phylogenetic analysis with the most complete taxon sampling of the subgenera *Cryptocambeva* and *Paracambeva*; and delimitation of areas of endemism potentially relevant for conservation priority strategies in a tropical mountain region.



**Citation:** Costa, W.J.E.M.; Azevedo-Santos, V.M.; Mattos, J.L.O.; Katz, A.M. Molecular Phylogeny, Taxonomy and Distribution Patterns of Trichomycterine Catfishes in the Middle Rio Grande Drainage, South-Eastern Brazil (Siluriformes: Trichomycteridae). *Fishes* **2023**, *8*, 206. <https://doi.org/10.3390/fishes8040206>

Academic Editors: Joseph Quattro and William B. Driggers

Received: 22 March 2023

Revised: 10 April 2023

Accepted: 13 April 2023

Published: 15 April 2023



**Copyright:** © 2023 by the authors. Licensee MDPI, Basel, Switzerland. This article is an open access article distributed under the terms and conditions of the Creative Commons Attribution (CC BY) license (<https://creativecommons.org/licenses/by/4.0/>).

## 1. Introduction

The Rio Grande drainage, with about 160,000 km<sup>2</sup>, is one of the main sources of the Rio de La Plata system, the fourth largest river basin in the world. Its main source is located in the Serra da Mantiqueira, at about 2000 m asl, but the presence of numerous tributaries with headwaters in different isolated mountain ranges makes the region a promising site for diversification of fish adapted for life in mountain fast-flowing rivers [1]. This drainage also plays a key role in supplying water and electricity to the main Brazilian urban centres, and as a result, its watercourses have been the target of constant human interventions, including 12 large dams and numerous small impoundments for energy production [2,3].

Much of what is known about the ichthyofauna of the Rio Grande drainage is related to environmental studies associated with the construction of various hydroelectric plants. These studies mainly focused on the diversified fauna of medium- and large-sized fish, as they are of relevant importance in regional economy [2–4]. However, the small fish fauna, particularly that inhabiting streams, remained little studied until recently [5], with many

species being described in recent years [1,6–11]. On the other hand, small-sized species with distribution restricted to segments of the drainage in high areas, such as the species of the group studied here, are particularly susceptible to extinction in a scenario of large human interventions, such as that in course in the Rio Grande drainage, therefore deserving special attention.

Among the little studied fish groups in the Rio Grande basin are the Trichomycterinae (hereafter trichomycterines), which are typical mountain-stream dwellers. Trichomycterines have a wide distribution throughout South America [12], but often show a high concentration of endemic species in relatively small mountainous areas [13–18]. In the Rio Grande drainage, trichomycterines belong to two groups, the subgenera *Cryptocambeva* Costa, 2021, and *Paracambeva* Costa, 2021, of the genus *Trichomycterus* Valenciennes, 1832. Species of these subgenera are often rare in ichthyological collections, probably due to their cryptic habits (e.g., burrowing habits in roots and leaves during daylight) and, consequently, are not easily sampled by usual collecting methods not causing environmental disturbs, as those used in the present study (i.e., small dip nets).

Our studies have shown that there is a clear limit in the distribution of trichomycterine species, with some species being endemic to the upper course of the Rio Grande and others being endemic to the middle course [1]. In the region of the middle course of the Rio Grande drainage (hereafter MRGD) between the middle-lower section of the Rio Sapucaí de Minas and the Rio Uberaba, the focal region of the present study, there are a total of two endemic species of *Cryptocambeva* [7,19] and two of *Paracambeva* [1,8]. However, our field studies have demonstrated an even greater diversity of species. Interestingly, our preliminary observations suggest that some species from the MRGD are more closely related to species from other regions than to other congeners endemic to the middle Rio Grande, as well as species from the MRGD representing different intrageneric groups may have similar distribution patterns. The objectives of the present study are to determine the genetic relationships among species from the MRGD and establish their possible relationships with species from other regions; to describe the new species; to discuss species distribution patterns, delimiting areas of endemism as priority areas for conservation; and to provide an identification key to the trichomycterine species from the MRGD.

## 2. Materials and Methods

### 2.1. Specimens

The specimens were collected using dip nets. Field collections were conducted with collecting permits given by the ICMBio (Instituto Chico Mendes de Conservação da Biodiversidade; permit numbers: 38553-13) and methods approved by the CEUA-CCS-UFRJ (Ethics Committee for Animal Use of the Federal University of Rio de Janeiro; permit number: 065/18), including euthanasia that followed the AVMA Guidelines for the Euthanasia of Animals [20], using a buffered solution of tricaine methane sulphonate (MS-222) at a concentration of 250 mg/L, or eugenol solution. The specimens used in the morphological studies were fixed in formalin for two weeks and then transferred into 70% ethanol, whereas the specimens used in the molecular analysis were fixed and preserved in absolute ethanol. The osteological preparations followed [21]; in the lists of the materials examined, the abbreviation C&S indicates cleared and stained specimens. Most specimens used in this study were deposited in the Instituto de Biologia, Universidade Federal do Rio de Janeiro (UFRJ), with a few samples deposited in the Centro de Ciências Agrárias e Ambientais, Universidade Federal do Maranhão (CICCAA). Some specimens previously deposited in other institutions were also examined, including Museu Nacional, Rio de Janeiro (MNRJ), and Museu de Zoologia, Universidade do Estado de São Paulo, São Paulo (MZUSP). Along the text, geographical names always correspond to the Portuguese names used in the region. A list of comparative materials appears in [1,22].

## 2.2. Morphological Data

The measurements followed landmarks proposed by Costa [23], with modifications added in Costa et al. [24]. The measurements were presented as percentages of standard length (SL) or head length. Only well-preserved specimens, which were fixed in formalin and with 30 mm SL or more, were measured. In the species descriptions, fin-ray counts were expressed using the formulae described by Costa et al. [24], which follow standards described in Bockmann and Sazima [25]. The vertebral counts included all elements, except the Apparatus of Weber. Osteological illustrations were prepared based on drafts of dissected cleared and stained specimens, which were directly made in a stereomicroscope Zeiss Stemi SV 6 with camera lucida. The terminology for osteological structures follows Costa [26], and for pores of the latero-sensory system, it follows Arratia and Huaquin [27], with modifications proposed by Bockmann and Sazima [25].

## 2.3. DNA Extraction, Amplification, and Sequencing

The genomic DNA was extracted from the muscle tissue taken from the right side of the caudal peduncle using a DNeasy Blood & Tissue Kit (Qiagen). The DNA extract quality was evaluated by agarose gel electrophoresis. Polymerase chain reaction (PCR) was used to amplify the target DNA sequences. The following primers were used: for mitochondrial encoded genes, Glu 31 [28] and Cytb Siluri R [29] for *cytochrome b* (CYTB), and FISHF1 and FISHR1 [30] for *cytochrome c oxidase I* (COX1), along with RAG2 TRICHO F and RAG2 TRICHO R [31] for the nuclear encoded gene *recombination-activating 2* (RAG2). The PCR reactions were carried out in 60 µL as follows: 5× GreenGoTaq Reaction Buffer (Promega), 1.5 mM MgCl<sub>2</sub>, 1 µM of each primer, 0.2 mM of each dNTP, 1 u of Promega GoTaq Hot Start polymerase, and 50 ng of genomic DNA. All reactions included negative controls to check for contaminants. The thermal profile of the PCR protocol was as follows: denaturation for 2–5 min at 95 °C; 35 cycles of denaturation for 1 min at 94–95 °C, annealing for 0.5–1 min at 45–55 °C, extension for 1–1.2 min at 72 °C, and final extension for 7 min at 72 °C. The PCR products were purified using the Wizard SV Gel and PCR Clean-Up System (Promega). The sequencing reactions in both directions were made using the BigDye Terminator Cycle Sequencing Mix (Applied Biosystems). The cycle sequencing reactions were performed in 20 µL reaction volumes containing 4 µL of BigDye, 2 µL of sequencing buffer 5× (Applied Biosystems), 2 µL of the amplified products (30–40 ng), 2 µL of the primer, and 10 µL of deionised water. The thermal profile was 35 cycles of 10 s at 96 °C, 5 s at 54 °C, and 4 min at 60 °C. Reading and interpretation of sequencing chromatograms and sequence annotation were performed using MEGA 11 [32]. The DNA sequences were translated into amino acid residues using the program MEGA 11 to verify the codification of each gene sequence and the absence of premature stop codons or indels. The GenBank accession numbers are provided in Appendix A.

## 2.4. Phylogenetic Analyses

A total of 43 terminal taxa were used in the phylogenetic analysis. The focus of the analysis were species of *Cryptocambeva* and *Paracambeva*, the only trichomycterine taxa occurring in the study area. The taxon sampling, thus, comprised the most complete sample of species of *Cryptocambeva* and *Paracambeva* in phylogenetic studies, including 15 of the 17 valid species and 3 new species of *Cryptocambeva* recognised here and all of the 11 valid species and 2 new species of *Paracambeva* described here. Only *Trichomycterus* (*Cryptocambeva*) *giarettai* Barbosa & Katz, 2016, *Trichomycterus* (*Cryptocambeva*) *maracaya* Bockmann & Sazima, 2004, and one new species of *Cryptocambeva* described here were not included in the phylogenetic analysis since tissues for DNA extraction were not available. In addition, the analysis also included the two valid species of the subgenus *Humboldtglanis* Costa, 2021, the sister group of *Cryptocambeva* [26], and one species of the subgenus *Trichomycterus*. The outgroups were four trichomycterines representing other subfamilial lineages, with two species representing other trichomycterid subfamilies; two species representing other loricarioid lineages; and one species representing a basal siluriform lineage (Appendix A).

The analysis included DNA sequences generated by us and others taken from GenBank, which were first generated in previous studies (e.g., [16,22]). Separate gene datasets were aligned using the Clustal W algorithm [33] in MEGA 11. No gaps or stop codons were identified. The concatenated molecular data matrix was composed of 2600 bp (COX1 752 bp, CYTB 1029 bp, and RAG2 819 bp). The PartitionFinder2.1.1 algorithm [34] was used to calculate the optimal partition scheme and best-fit evolutive models based on the Corrected Akaike Information Criterion (Appendix B). Two independent approaches for phylogenetic reconstruction were implemented, Bayesian Inference (BI) and Maximum Likelihood (ML). BI was conducted using Beast 1.10.4 [35]. A Birth-Death speciation process was used as the tree prior [36]. Two independent Markov chain Monte Carlo (MCMC) runs with  $5 \times 10^7$  generations were run with a sampling frequency of 1000 generations. Convergence of the MCMC chains, attainment of the stationary phase, effective sample size adequacy, and determination of the proper burn-in value were evaluated using Tracer 1.7.1. [37]. To produce the consensus tree and calculate Bayesian posterior probabilities, we utilized Tree Annotator v.1.10.4 applying a 25% burn-in. The ML analysis was performed using IQ-TREE 2.2.0 [38], and node support was assessed using both ultrafast bootstrap [39] and bootstrap [40] algorithms, each with 1000 replicates.

### 3. Results

#### 3.1. Molecular Phylogeny

The phylogenetic analyses generated identical trees (Figure 1). Both *Cryptocambeva* and *Paracambeva* are corroborated as monophyletic with highest support values. In each subgenus, species endemic to the MRGD do not form a single monophyletic group (see discussion below).

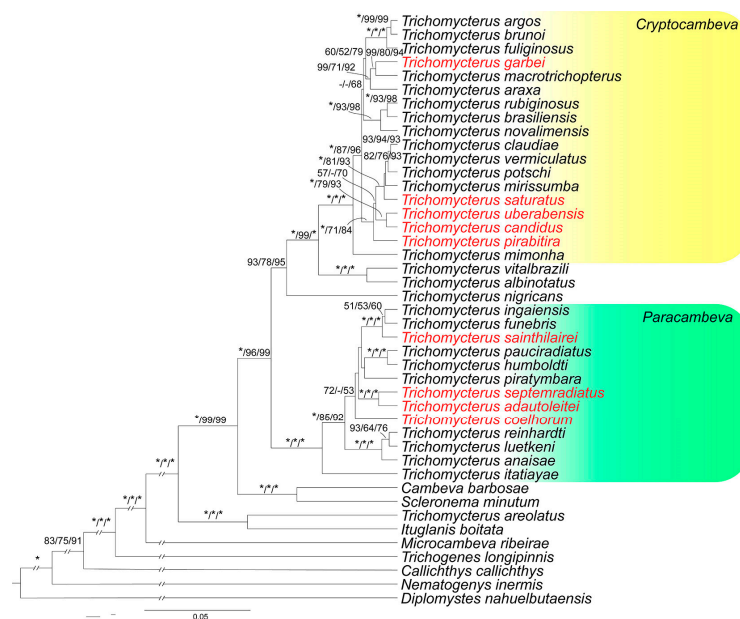


**Figure 1.** Bayesian Inference tree estimated by Beast for 47 taxa, using 3 genes (COI, CYTB, and RAG2), with a total of 2600 bp. The numbers above the branches indicate Bayesian posterior probabilities of the Bayesian Inference analysis, and bootstrap and fast bootstrap values of the Maximum Likelihood analyses, respectively, separated by bars. Asterisks (\*) indicate maximum support values, and dashes (-) indicate values below 50. Taxa in red are species from the Middle Rio Grande drainage.

#### 3.2. Taxonomic Accounts

##### 3.2.1. Subgenus *Cryptocambeva* Costa, 2021

Species of *Cryptocambeva* may be diagnosed by a series of apomorphic conditions, including a small posttemporo-supracleithrum, resulting in a broad interspace between the posttemporo-supracleithrum and adjacent bones, and a colour pattern consisting of

small dark brown to black dots scattered over all the body [26,41]. *Cryptocambeva* and its sister group, the subgenus *Humboldtglanis* Costa, 2021, share a series of synapomorphies, including the presence of a long and narrow ridge on the dorsal surface of the autopalatine, the ventral surface of the lateral margin of the mesethmoid being ventrally folded around the vomer margin, and the lateral ethmoid being medially separated from its symmetrical homologous by an interspace. Species of *Cryptocambeva* are easily distinguished from species of *Humboldtglanis* by species of the former subgenus having six or seven pectoral-fin rays (vs. always eight). In the MRGD, two morphological patterns are present: a clade herein called the *Trichomycterus candidus* complex, which contains three small species not surpassing about 60 mm SL and lacking pelvic fin and girdle (see discussion below), and an assemblage comprising three species not forming a monophyletic group, but sharing well-developed pelvic fin and girdle and a relatively robust body, often reaching about 100–120 mm SL. Species of the *Trichomycterus candidus* complex are typically found among leaves of amphibious plants, thus contrasting with other congeners that are commonly found deeply buried in riverbanks, often close to marginal plant roots or within bottom leaf litter.

*Trichomycterus (Cryptocambeva) candidus* (Miranda Ribeiro, 1949)

Figure 2

*Eremophilus candidus* Miranda Ribeiro, 1949: [19] (2) (original description; type locality: ‘pequeno córrego que cai no ribeirão Espírito Santo [21°05′44″ S 46°08′46″ W], afluente do Rio Claro e este do Sapucaí, que desagua no Rio Grande, Município de Conceição Aparecida, Estado de Minas Gerais’ [small stream that flows into the Ribeirão Espírito Santo, a tributary of the Rio Claro, which is tributary of the Sapucaí, which flows into the Rio Grande, Municipality of Conceição Aparecida, State of Minas Gerais]; holotype: MNRJ 5209).

*Trichomycterus candidus*: [41] (180) (new combination).

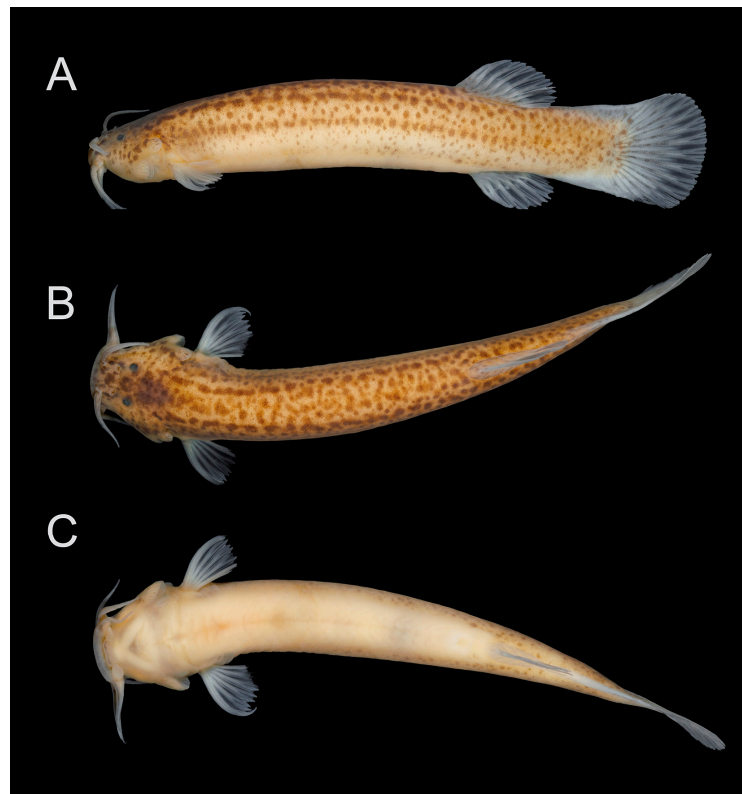


**Figure 2.** *Trichomycterus candidus*, UFRJ 12824, Conceição da Aparecida Municipality, 43.1 mm SL: (A) lateral, (B) dorsal, and (C) ventral views.

**Diagnosis.** *Trichomycterus candidus* differs from all other congeners of *Cryptocambeva*, except for *Trichomycterus listruoides* Costa, Katz & Azevedo-Santos sp. nov. and *Trichomycterus uberabensis* Costa, Azevedo-Santos & Katz sp. nov., by the pelvic fin and girdle that are absent in most specimens, or rudimentary in two specimens (UFRJ 12728, see discussion below), in contrast to being always well developed. *Trichomycterus candidus* differs from *T. listruoides* Costa, Katz & Azevedo-Santos sp. nov. and *T. uberabensis* Costa, Azevedo-Santos & Katz sp. nov. by having a unique colour pattern, comprising minute dark brown dots, which are equal to or smaller than the orbital diameter, irregularly arranged over the flank, and separated by broad interspaces; a horizontal row of slightly larger dark brown dots along the longitudinal midline of the flank; and another similar horizontal row on the dorsal portion of the flank (vs. flank dots always larger than the orbital diameter, forming a vermiculate pattern in *T. listruoides*, and small round spots in *T. uberabensis*). *Trichomycterus candidus* is also distinguished from *T. listruoides* Costa, Katz & Azevedo-Santos sp. nov. by having a caudal fin margin not aligned with the caudal peduncle (vs. in a continuous line); fewer dorsal (19 or 20 vs. 24 or 25) and ventral (17 or 18 vs. 20) procurrent caudal-fin rays; fewer vertebrae (38 or 39 vs. 40); dorsal-fin origin at the vertical between the centrum of the 22nd or 23rd vertebra (vs. 24th); and anal-fin origin at vertical through the centrum of the 25th vertebra (vs. 26th or 27th). It is also distinguished from *T. uberabensis* by having more ventral procurrent caudal-fin rays (17 or 18 vs. 13–16), fewer interopercular odontodes (16–19, vs. 21–24), and fewer teeth on the dentary (21–25, vs. 29–32). For a full description and anatomical illustrations, see Barbosa and Costa [41].

**Distribution.** *Trichomycterus candidus* occurs in the western tributaries of the Rio Sapucaí, Rio Grande drainage, upper Rio Paraná basin (Figure 3B), at altitudes of about 800 m asl. Specimens from two populations, one from Ribeirão Antinha, Capetinga, and another from the Rio Itaci, an eastern tributary of the Rio Sapucaí (Figure 3B), were tentatively identified as *Trichomycterus* cf. *candidus*. Specimens from these populations are similar to *T. candidus*, except for some smaller specimens from the Ribeirão Antinha having a distinct colour pattern (i.e., dots coalesced to form two stripes on the flank), fewer vertebrae (37 vs. 38–39), and more opercular odontodes (12 or 13 vs. 8–10), and specimens from the Rio Itaci having flank dots not forming distinctive rows (vs. two distinctive longitudinal rows).

**Material examined.** *Trichomycterus (Cryptocambeva) candidus*: all localities in Brazil: Minas Gerais State: Rio Grande drainage, Rio Paraná basin. Conceição da Aparecida Municipality: MNRJ 5209, holotype; stream tributary of Rio Claro, with itself being a tributary of Rio Sapucaí, 21°05'44" S 46°08'46" W; J. C. M. Carvalho & C. Lako, October 1947. MNRJ 5356, 21 ex.; Renascença Farm; J. C. M. Carvalho & A. L. de Castro, November 1948. UFRJ 4926, 31 ex.; UFRJ 4928, 5 ex. (C&S); Riacho Cuiabá; D. Almeida, M. P. Gonçalves & M. A. Barbosa, 24 October 1999. UFRJ 12824, 6; stream near the road MG-184, 21°03'25" S 46°08'55" W, at about 800 m asl; A. M. Katz & V.M. de Azevedo Santos, 30 October 2021. Carmo do Rio Claro Municipality: UFRJ 12728, 15 ex.; Ribeirão Santa Quitéria, Cachoeira da Pedra Molhada, 21°00'18" S 46°14'49" W, at about 810 m asl; V.M. Azevedo-Santos et al., 21 July 2017. UFRJ 12826, 4 ex.; same locality as UFRJ 12728; A. M. Katz & V.M. Azevedo-Santos, 30 October 2021. *Trichomycterus (Cryptocambeva) cf. candidus* 1: UFRJ 8384, 16 ex.; 8391, 3 ex. (C&S); Capetinga Municipality: stream tributary of Ribeirão Antinha, Rio Grande drainage, Rio Paraná basin, 20°38'23" S 46°59'02" W, altitude about 750 m asl; V.M. Azevedo-Santos, 4 November 2011. UFRJ 8372, 5 ex.; same locality and collector as preceding, 21 August 2011. *Trichomycterus (Cryptocambeva) cf. candidus* 2: UFRJ 12823, 2 (C&S); stream tributary of Rio Itaci, a tributary of Rio Sapucaí, Rio Grande drainage, upper Rio Paraná basin, 20°54'58" S 45°56'21" W, about 840 m asl; A. M. Katz & V. M. Azevedo-Santos, 31 October 2021. UFRJ 12825, 2 ex.; same locality as preceding; A. M. Katz & V.M. Azevedo-Santos, 31 October 2021.

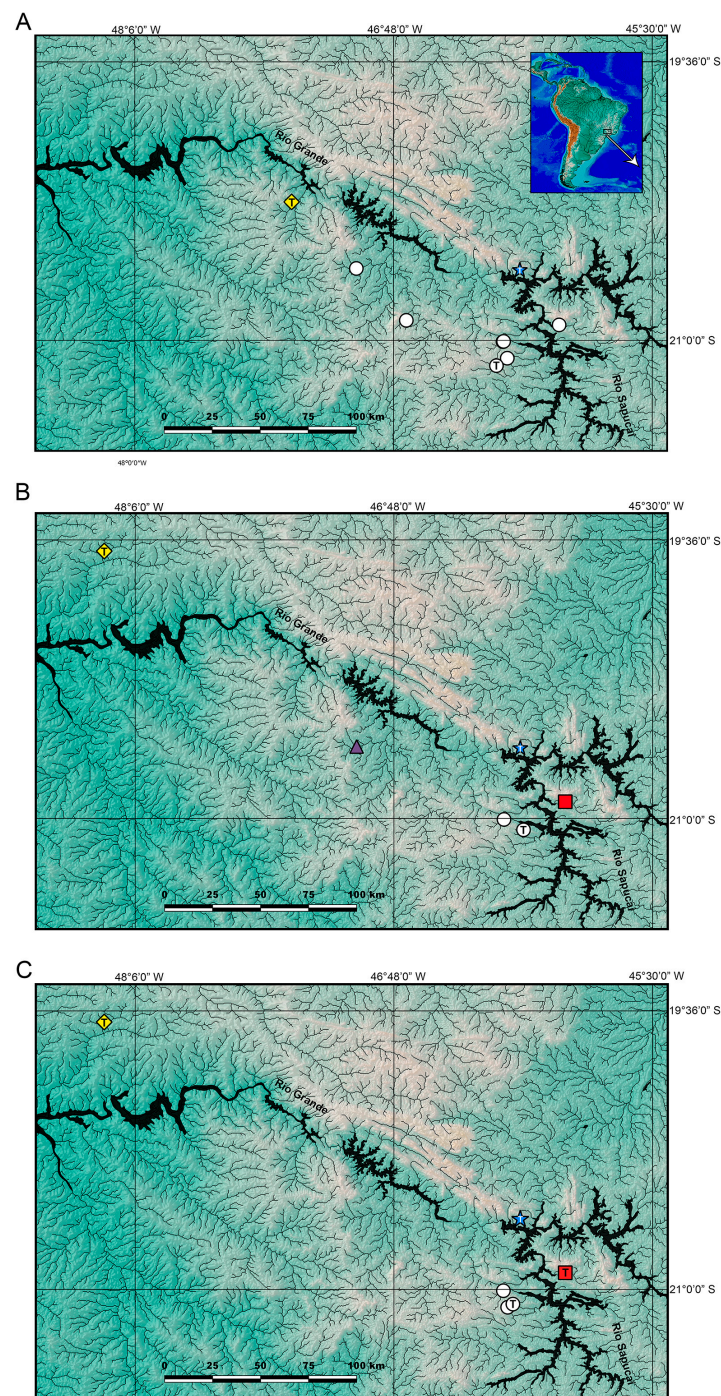


**Figure 3.** Geographical distribution of *Trichomycterus* in the Middle Rio Grande drainage. **(A)** *T. garbei* Costa, Azevedo-Santos & Katz sp. nov. (triangle), *T. pirabityra* (dots), and *T. saturaturatus* Costa, Katz & Azevedo-Santos sp. nov. (star); **(B)** *T. candidus* (dots), *T. cf. candidus* 1 (triangle), *T. cf. candidus* 2 (square), *T. listruoides* Costa, Katz & Azevedo-Santos sp. nov. (star), and *T. uberabensis* Costa, azevedo-Santos & Katz sp. nov. (lozenge); **(C)** *T. adautoleitei* Costa, Azevedo-Santos & Katz sp. nov. (square), *T. coelhorum* Costa, Azevedo-Santos & Katz sp. nov. (lozenge), *T. sainthilairei* (star), and *T. septemradiatus* (dots). T indicates type localities.

*Trichomycterus (Cryptocambeva) garbei* Costa, Azevedo-Santos & Katz sp. nov.  
 LSID: urn:lsid:zoobank.org:act:4F240F1F-C0F4-40D0-9778-6C2B9521F799  
 Figures 4, 5A, 6A and 7A; Table 1



**Figure 4.** *Trichomycterus (Cryptocambeva) garbei* Costa, Azevedo-Santos & Katz sp. nov. Holotype, UFRJ 12824, Cristais Paulista Municipality, 60.8 mm SL: (A) lateral, (B) dorsal, and (C) ventral views.

*Holotype.* UFRJ 12917, 60.8 mm SL; Brazil: São Paulo State: Cristais Paulista Municipality: stream tributary of Rio Canoas, which is a tributary of Rio Grande at Estreito dam, road Cristais Paulista to Mascarenhas, 20°18'07''S 47°18'45''W, at about 715 m asl; V. M. Azevedo-Santos et al., 16 April 2022.

*Paratypes.* UFRJ 12918, 11 ex., 32.3–70.5 mm SL; UFRJ 12960, 3 ex., 38.8–53.3 mm SL (C&S); CICCAA 07645, 4 ex., 42.6–49.6 mm SL; UFRJ 12896, 9 ex. (DNA), 34.3–62.5 mm SL; collected with holotype.

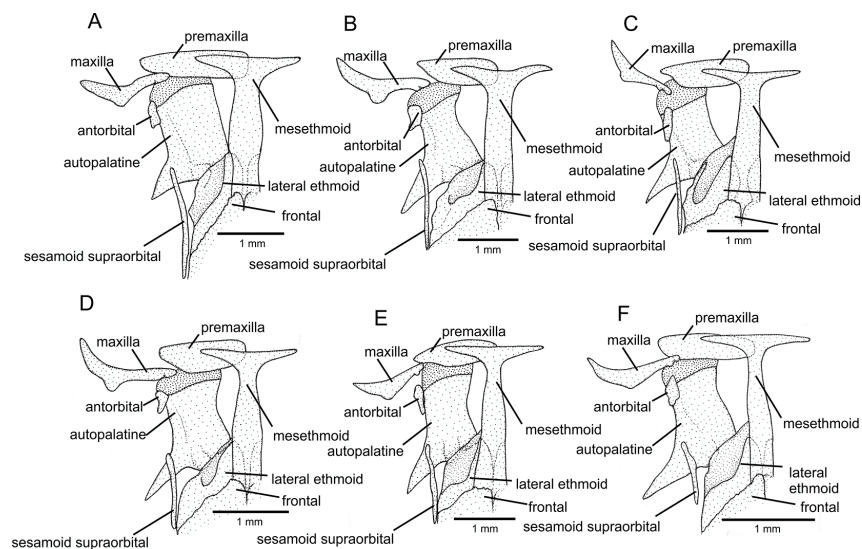


**Figure 5.** Mesethmoidal region, with middle and left portions, and in dorsal view: (A) *Trichomycterus (Cryptocambeva) garbei* Costa, Azevedo-Santos & Katz sp. nov.; (B) *Trichomycterus (Cryptocambeva) listruoides* Costa, Katz & Azevedo-Santos sp. nov.; (C) *Trichomycterus (Cryptocambeva) saturatus* Costa, Katz & Azevedo-Santos sp. nov.; (D) *Trichomycterus (Cryptocambeva) uberabensis* Costa, Azevedo-Santos & Katz sp. nov.; (E) *Trichomycterus (Paracambeva) adautoleitei* Costa, Azevedo-Santos & Katz sp. nov.; and (F) *Trichomycterus (Paracambeva) coelhorum* Costa, Azevedo-Santos & Katz sp. nov. Larger stippling represents cartilage.

**Diagnosis.** *Trichomycterus garbei* is distinguished from all other congeners of the subgenus *Cryptocambeva* by possessing a dorsally expanded caudal peduncle as a result of long and numerous dorsal procurrent caudal-fin rays (29–32 vs. 15–25). Additionally, it is distinguished from other species of *Cryptocambeva* from the Rio Grande drainage by a combination of the presence of well-developed pelvic fin and girdle (vs. absence in species of the *T. candidus* complex), the absence of the anterior segment of the infraorbital canal (vs. presence in *T. pirabitira* and *T. saturatus* Costa, Katz & Azevedo-Santos sp. nov.), and 19 or 20 ventral procurrent caudal-fin rays (vs. 13–18 in *T. pirabitira* and *T. saturatus*).

**Description.** General morphology: Morphometric data are presented in Table 1. Body relatively deep, compressed. Greatest body depth in area immediately anterior to pelvic-fin base, or sometimes at middle portion of caudal peduncle. Dorsal and ventral profiles slightly convex between snout and anterior limit of caudal peduncle. Dorsal margin of caudal peduncle slightly expanded on its middle portion resulting in convex dorsal profile; ventral profile of caudal peduncle nearly straight. Anus and urogenital papilla opening at vertical just anterior to middle portion of dorsal-fin base. Head sub-trapezoidal in dorsal view, with anterior profile of snout convex. Eye small, dorsally positioned on head, nearer snout tip than posterior margin of opercle. Posterior nostril nearer anterior nostril than orbit. Tip of nasal barbel posteriorly reaching area between orbit and opercle, sometimes reaching middle of opercle; tip of maxillary barbel reaching between middle of interopercular patch of odontodes and area between interopercle and pectoral-fin base; rictal barbel reaching between middle and posterior portion of interopercular patch of odontodes. Mouth subterminal. Jaw teeth pointed, irregularly arranged, 46–70 on premaxilla, 50–59 on dentary. Minute skin papillae on dorsal and ventral surfaces of head. Branchial membrane attached to isthmus only at its anterior-most point, in ventral midline.

**Table 1.** Morphometric data of *Trichomycterus garbei* Costa, Azevedo-Santos & Katz sp. nov.

	Holotype	Paratypes (n = 10)
Standard length (SL)	60.8	43.6–70.5
<b>Percentage of standard length</b>		
Body depth	17.1	15.6–20.1
Caudal peduncle depth	17.3	14.9–17.6
Body width	10.9	9.8–12.9
Caudal peduncle width	2.9	2.2–3.2
Pre-dorsal length	63.6	58.7–63.8
Pre-pelvic length	59.7	55.9–59.3
Dorsal-fin base length	12.0	10.4–12.9
Anal-fin base length	10.2	9.0–11.4
Caudal-fin length	17.6	17.4–19.9
Pectoral-fin length	13.8	13.6–15.8
Pelvic-fin length	9.4	8.9–10.7
Head length	20.0	18.8–21.2
<b>Percentage of head length</b>		
Head depth	49.3	44.0–51.5
Head width	88.7	81.6–89.7
Snout length	40.1	38.1–44.5
Interorbital width	28.3	23.9–29.4
Preorbital length	12.6	10.0–13.3
Eye diameter	9.2	9.0–11.8

Dorsal and anal fins subtriangular. Total dorsal-fin rays 11 (ii + II + 7), total anal-fin rays 9 (ii + II + 5). Anal-fin origin at vertical through posterior portion of dorsal-fin base, at vertical through base of 5<sup>th</sup> bifid dorsal-fin ray. Dorsal-fin origin at vertical between

centrum of 16th and 18th vertebra; anal-fin origin at vertical between centrum of 20th and 22nd vertebra. Pectoral fin subtriangular in dorsal view, first pectoral-fin ray terminating in filament about 15–30 % pectoral-fin length excluding filament. Total pectoral-fin rays 7 (I + 6). Pelvic fin subtruncate, posteriorly overlapping anus and urogenital papilla, its posterior extremity at vertical just posterior to middle portion of dorsal-fin base. Pelvic-fin bases medially separated by small interspace, about one third of pelvic-fin base. Total pelvic-fin rays 5 (I + 4). Caudal fin subtruncate, posterior corners rounded. Total principal caudal-fin rays 13 (I + 11 + I), total dorsal procurent rays 29–32 (xxviii–xxxi + I), total ventral procurent rays 19 or 20 (xviii–xix + I).

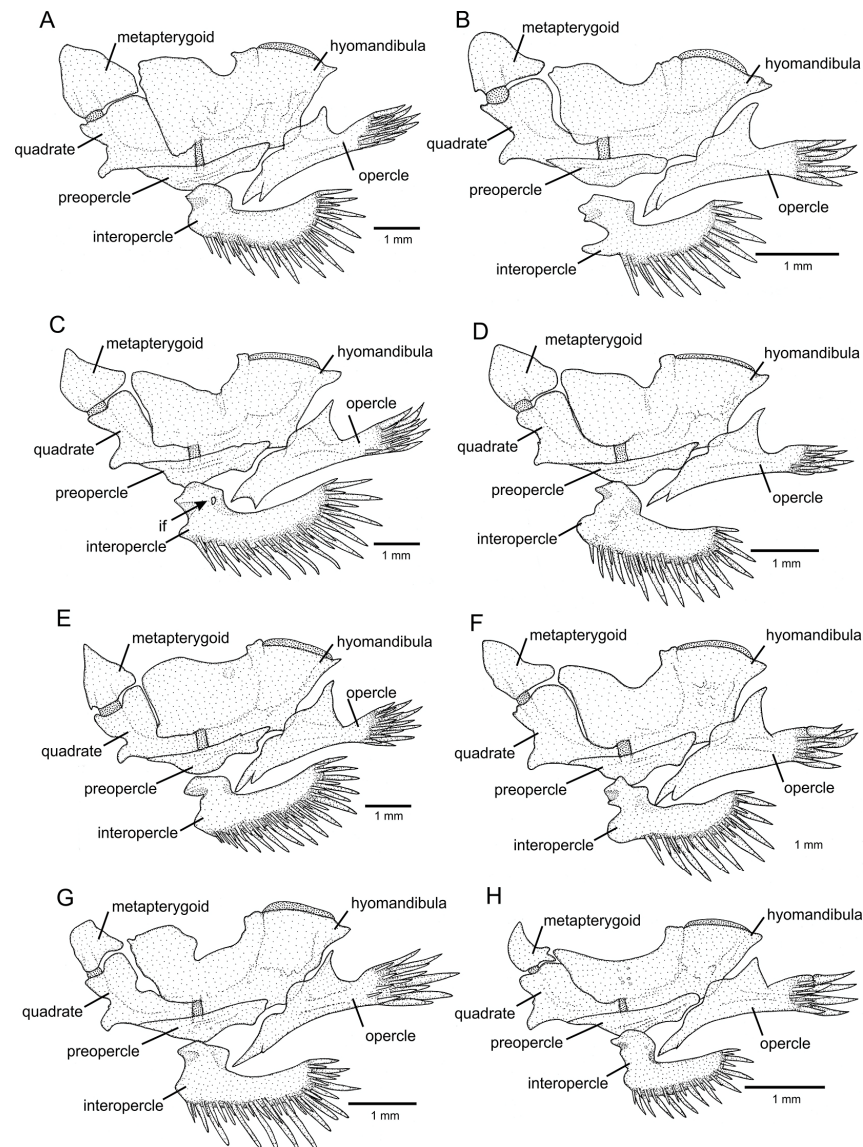


**Figure 6.** Left jaw suspensorium and opercular series, in lateral view: (A) *Trichomycterus (Cryptocambeva) garbei* Costa, Azevedo-Santos & Katz sp. nov.; (B) *Trichomycterus (Cryptocambeva) listruoides* Costa, Katz & Azevedo-Santos sp. nov.; (C) *Trichomycterus (Cryptocambeva) pirabitira*; (D) *Trichomycterus (Cryptocambeva) mirissumba*; (E) *Trichomycterus (Cryptocambeva) saturatus* Costa, Katz & Azevedo-Santos sp. nov.; (F) *Trichomycterus (Cryptocambeva) uberabensis* Costa, Azevedo-Santos & Katz sp. nov.; (G) *Trichomycterus (Paracambeva) adautoleitei* Costa, Azevedo-Santos & Katz sp. nov.; and (H) *Trichomycterus (Paracambeva) coelhorum* Costa, Azevedo-Santos & Katz sp. nov. Larger stippling represents cartilage.

Laterosensory system: Supraorbital, posterior section of infraorbital canal and postorbital canal continuous. Supraorbital sensory canal pores 3: s1, adjacent to medial margin of anterior nostril; s3, adjacent and just posterior to medial margin of posterior nostril; s6, in transverse line through posterior half of orbit; pore s6 slightly nearer its homologous pore than orbit. Anterior infraorbital sensory canal absent. Posterior infraorbital sensory canal pores 2: pore i10, adjacent to ventral margin of orbit, and pore i11, posterior to orbit. Postorbital canal pores 2: po1, at vertical through posterior portion of interopercular patch of odontodes, and po2, at vertical through posterior portion of opercular patch of odontodes. Lateral line pores 2; posterior-most pore at vertical just posterior to pectoral-fin base.

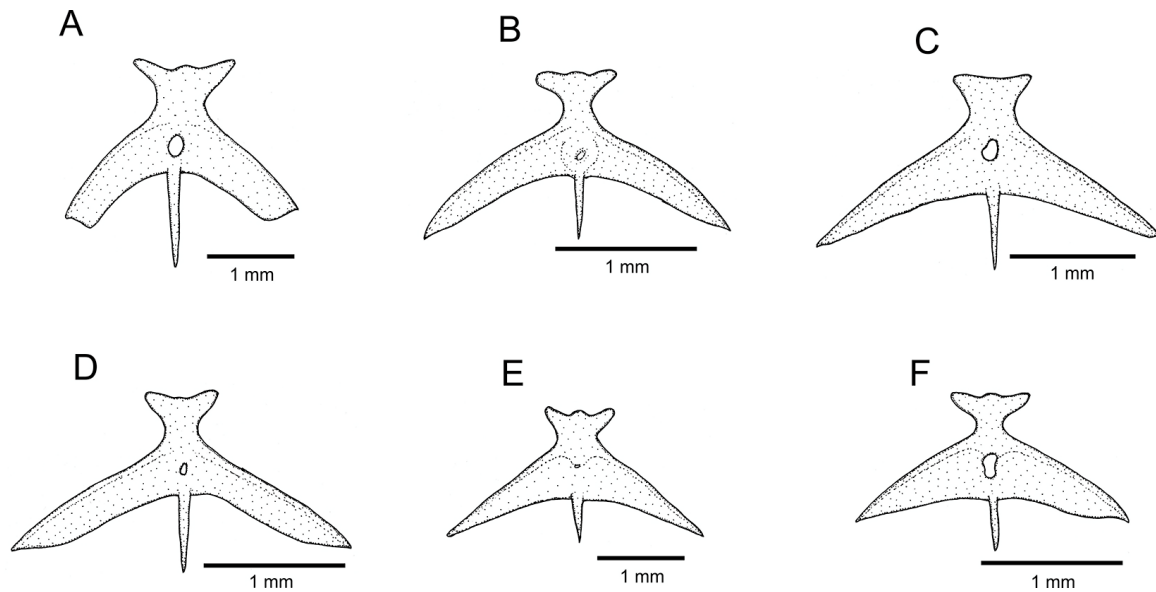


**Figure 7.** Parurohyal, in ventral view, of (A) *Trichomycterus (Cryptocambeva) garbei* Costa, Azevedo-Santos & Katz sp. nov.; (B) *Trichomycterus (Cryptocambeva) listruoides* Costa, Katz & Azevedo-Santos sp. nov.; (C) *Trichomycterus (Cryptocambeva) saturatus* Costa, Katz & Azevedo-Santos sp. nov.; (D) *Trichomycterus (Cryptocambeva) uberabensis* Costa, Azevedo-Santos & Katz sp. nov.; (E) *Trichomycterus (Paracambeva) adautoleitei* Costa, Azevedo-Santos & Katz sp. nov.; and (F) *Trichomycterus (Paracambeva) coelhorum* Costa, Azevedo-Santos & Katz sp. nov.

Osteology: Mesethmoid slender, anterior margin slightly about straight, main axis gradually widening posteriorly. Mesethmoid cornu narrow, tip rounded. Postero-lateral margin of lateral ethmoid with pronounced projection towards middle portion of sesamoid supraorbital. Antorbital thin, small, drop-shaped, separated from sesamoid supraorbital by interspace larger than antorbital length. Sesamoid supraorbital slender, without lateral projections, its length about four times antorbital length. Premaxilla sub-trapezoidal in dorsal view, long, longer than maxilla. Maxilla slightly curved. Autopalatine sub-rectangular in dorsal view when excluding its postero-lateral process, its largest width about two thirds of its length including anterior cartilage; medial margin about straight. Autopalatine posterolateral process well-developed, short, its length about half autopalatine length excluding anterior cartilage. Metapterygoid subtriangular, deeper than long, dorsal extremity blunt, anterior margin convex, posterior portion without distinctive posterior projection. Quadrate compact, dorsal margin with weak projection posterior to articulation to metapterygoid, anterodorsal tip slightly projected dorsally, posterodorsal margin in contact with hyomandibula outgrowth. Hyomandibula long, with well-developed anterior outgrowth; dorsal margin of hyomandibula outgrowth with weak concavity on its posterior portion. Opercle long and slender, longer than interopercle. Opercular odontode patch slender, its width about half length of dorsal hyomandibula articular facet. Opercular odontodes 13–15, narrow, nearly straight, arranged in irregular transverse rows. Dorsal process of opercle short, subtriangular. Opercular articular facet for hyomandibula with

rounded lateral shield, articular facet for preopercle small, rounded. Interopercle moderate in length, about three fourths longitudinal length of hyomandibula, anterior portion convex; dorsal process placed near anterior margin of interopercle. Interopercular odontodes 28–32, nearly straight, pointed, arranged in irregular longitudinal rows. Preopercle compact, with minute ventral projection. Parurohyal robust, lateral process truncate, posteriorly curved. Parurohyal head well-developed, with pronounced anterolateral paired process. Middle parurohyal foramen elliptical. Posterior process of parurohyal long, approximately equal to distance between anterior margin of parurohyal and anterior insertion of posterior process. Branchiostegal rays 8. Vertebrae 34 – 36. Ribs 12. Two dorsal hypural plates corresponding to hypurals 3 + 4 + 5; single ventral hypural plate corresponding to hypurals 1 + 2 + parhypural.

Colouration in alcohol: Flank, dorsum and head side pale brown, densely covered by dark brown dots with size variable among specimens, since about half to four times orbit diameter; dots irregularly arranged. Venter and ventral surface of head white. Barbels pale brown. Fins pale brown to hyaline on extremities, with dark brown dots on basal region.

*Etymology.* The name *garbei* is in honour of Ernst Garbe (1853–1925), a German naturalist who was Brazilian naturalized and who, between 1882 and the period just before his death, travelled through several Brazilian regions, including the Rio Grande drainage, making a rich biological collection. He collected the type specimens of *Imparfinis longicauda* Borodin, 1927 [= *Heptapterus longicauda* (Borodin, 1927)] in the type locality of *T. garbei*.

*Distribution.* *Trichomycterus garbei* is only known from its type locality, a small stream tributary of the Rio Canoas, Rio Grande drainage, upper Rio Paraná basin, at about 715 m asl (Figure 3B).

*Trichomycterus (Cryptocambeva) listruoides* Costa, Katz & Azevedo-Santos sp. nov.

LSID: urn:lsid:zoobank.org:act: A9BAED1D-5828-4545-B9F8-CCA9A97D9358

Figures 5B, 6B, 7B and 8; Table 2

*Holotype.* UFRJ 11845, 55.1 mm SL; Brazil: Minas Gerais State: Capitólio Municipality: Córrego Tamborete, a tributary of Rio Grande at the Furnas dam, upper Rio Paraná basin, 20°38'53" S 46°09'55" W, about 875 m asl; A.M. Katz & P.H.N. Bragança, 14 February 2014.

*Paratypes.* UFRJ 10020, 4 ex., 30.8–56.2 mm SL; UFRJ 13345, 3 ex., 30.9–43.0 mm SL (C&S); CICCAA 07646, 2 ex., 42.7–42.9 mm SL; collected with holotype.

*Diagnosis.* *Trichomycterus listruoides* is distinguished from all other species of *Cryptocambeva*, except for *T. candidus* and *Trichomycterus uberabensis* Costa, Azevedo-Santos & Katz sp. nov., by the absence of pelvic fin and girdle (vs. presence). *Trichomycterus listruoides* differs from *T. candidus* and *T. uberabensis* Costa, Azevedo-Santos & Katz sp. Nov. by having the caudal fin margin aligned with the caudal peduncle, forming a spatula-like tail (vs. not aligned); more dorsal (24 or 25 vs. 17–20) and ventral (20 vs. 13–18) procurrent caudal-fin rays; fewer vertebrae (40 vs. 37–39); the dorsal-fin origin at the vertical between the centrum of the 24th vertebra (vs. 22nd or 23rd); the anal-fin origin at vertical through the centrum of the 26th or 27th vertebra (vs. 24th or 25th); and a vermiculate colour pattern on the flank (vs. minute dots in *T. candidus* and small round spots in *T. uberabensis*).

*Description.* General morphology: Morphometric data are presented in Table 2. Body relatively slender, subcylindrical anteriorly, compressed posteriorly. Greatest body depth in area approximately at midway between pectoral-fin base and anal-fin origin. Dorsal and ventral profiles slightly convex between snout and anterior limit of caudal peduncle, slightly convex on caudal peduncle due to slight expansion on area supported by procurrent caudal-fin rays. Anus and urogenital papilla opening at vertical just posterior dorsal-fin origin. Head sub-trapezoidal in dorsal view, with anterior profile of snout convex. Eye small, dorsally positioned on head, nearer snout tip than posterior margin of opercle. Posterior nostril nearer anterior nostril than orbit. Tip of nasal barbel posteriorly reaching area just anterior to orbit; tip of maxillary barbel reaching between interopercular patch of odontodes and pectoral-fin base; rictal barbel reaching posterior portion of interopercular patch of odontodes. Mouth subterminal. Jaw teeth pointed, irregularly arranged, 19–26 on premaxilla, 22–25 on dentary. Minute skin papillae on snout and ventral surface of head.

Branchial membrane attached to isthmus only at its anterior-most point, in ventral midline.

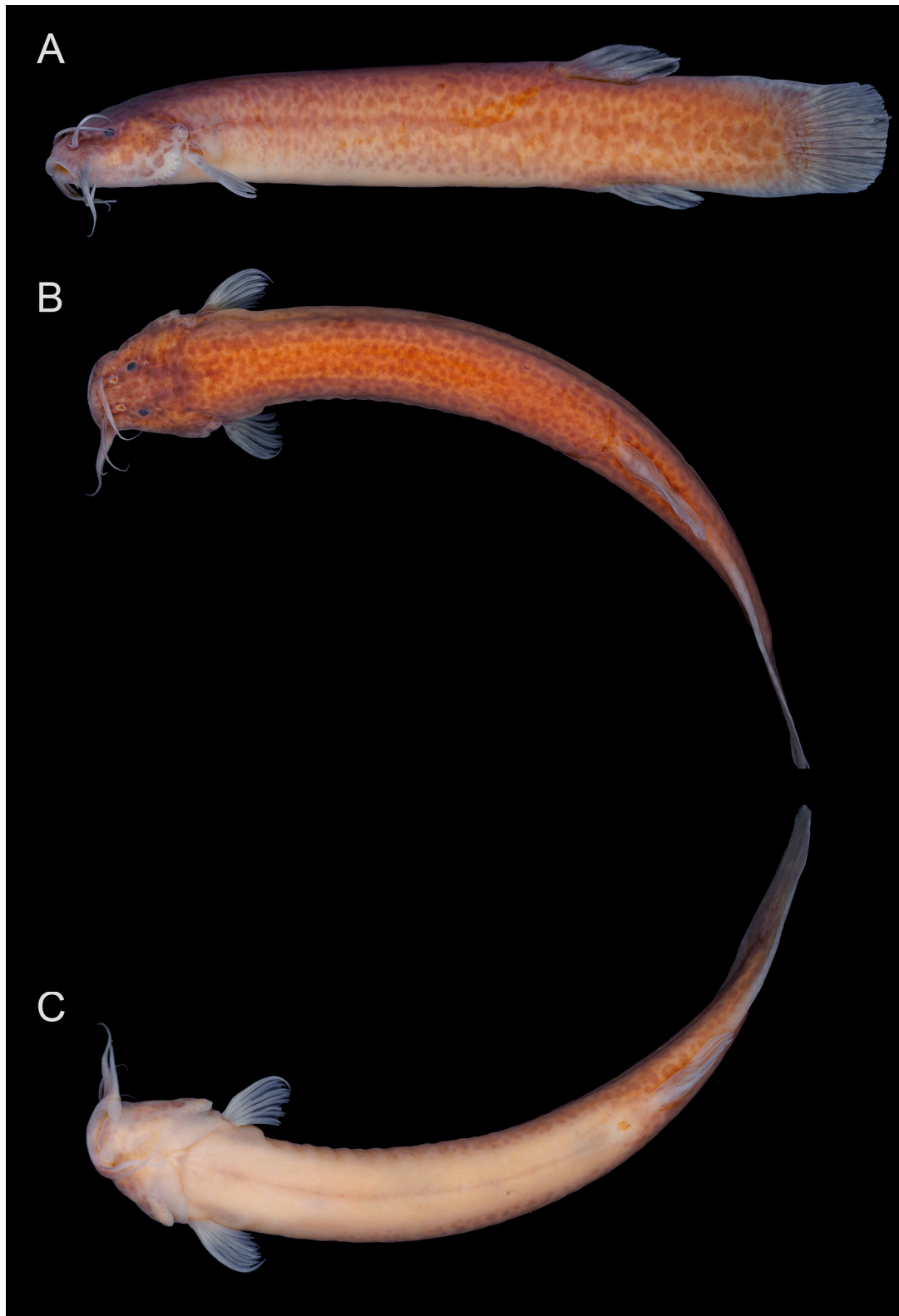


**Figure 8.** *Trichomycterus (Cryptocambeva) listruoides* Costa, Katz & Azevedo-Santos sp. nov. Holotype, UFRJ 11845, Capitólio, 55.1 mm SL: (A) lateral, (B) dorsal, and (C) ventral views.

Dorsal and anal fins rounded, dorsal fin slender, longest ray shorter than anal-fin base length. Total dorsal-fin rays 11 (ii + II + 7), total anal-fin rays 9 (ii + II + 5). Anal-fin origin at vertical through middle portion of dorsal-fin base, or slightly anterior to it, at vertical through base of 5th segmented dorsal-fin ray. Dorsal-fin origin at vertical through centrum of 24th vertebra; anal-fin origin at vertical between centrum of 26th and 27th vertebra. Pectoral fin subtriangular in dorsal view, first pectoral-fin ray terminating in filament about 20–30 % pectoral-fin length excluding filament. Total pectoral-fin rays 6 (I + 5). Pelvic fin and girdle absent. Caudal fin rounded, continuous with caudal peduncle, forming spatula-shaped tail. Total principal caudal-fin rays 13 (I + 11 + I), total dorsal procurent rays 24 or 25 (xxiii–xxiv + I), total ventral procurent rays 20 (xix + I).

**Table 2.** Morphometric data of *Trichomycterus listruoides* Costa, Katz & Azevedo-Santos sp. nov.

	Holotype	Paratypes ( <i>n</i> = 5)
Standard length (SL)	55.1	42.6–56.2
<b>Percentage of standard length</b>		
Body depth	18.1	11.3–18.1
Caudal peduncle depth	16.0	10.5–16.0
Body width	10.3	7.4–10.3
Caudal peduncle width	3.3	2.5–3.3
Pre-dorsal length	67.3	52.3–67.3
Dorsal-fin base length	11.8	9.1–11.8
Anal-fin base length	8.7	7.4–8.9
Caudal-fin length	20.3	15.1–20.7
Pectoral-fin length	11.1	7.6–11.1
Head length	17.2	13.2–17.2
<b>Percentage of head length</b>		
Head depth	54.7	43.2–54.7
Head width	84.2	64.2–84.2
Snout length	36.8	31.6–42.1
Interorbital width	28.4	22.1–28.4
Preorbital length	12.6	8.4–12.6
Eye diameter	8.4	7.3–9.3

Laterosensory system: Supraorbital, posterior section of infraorbital canal and postorbital canal continuous. Supraorbital sensory canal pores 3: s1, adjacent to medial margin of anterior nostril; s3, adjacent and just posterior to medial margin of posterior nostril; s6, in transverse line through posterior half of orbit; pore s6 approximately equidistant from its homologous pore and adjacent orbit. Anterior infraorbital sensory canal absent. Posterior infraorbital sensory canal pores 2: pore i10, adjacent to ventral margin of orbit, and pore i11, posterior to orbit. Postorbital canal pores 2: po1, at vertical through posterior portion of interopercular patch of odontodes, and po2, at vertical through posterior portion of opercular patch of odontodes. Lateral line pores 2; posterior-most pore at vertical just posterior to pectoral-fin base.

Osteology: Mesethmoid slender, anterior margin slightly concave, main axis gradually widening posteriorly. Mesethmoid cornu narrow, slightly curved posteriorly, extremity pointed. Postero-lateral margin of lateral ethmoid with small projection. Antorbital thin, small, drop-shaped, separated from sesamoid supraorbital by interspace larger than antorbital length. Sesamoid supraorbital slender, without lateral projections, its length about four times antorbital length. Premaxilla sub-trapezoidal in dorsal view, laterally tapering, shorter than maxilla. Maxilla slightly curved. Autopalatine sub-rectangular in dorsal view when excluding its postero-lateral process, its largest width about half its length

including anterior cartilage; medial margin concave. Autopalatine posterolateral process well-developed, its length slightly larger than autopalatine largest width. Metapterygoid subtriangular to subtrapezoidal, longer than deep, dorsal extremity rounded or truncate, anterior margin convex, with small ventral projection, posterior portion with distinctive posterior projection. Quadrate compact, dorsal margin with weak projection posterior to articulation to metapterygoid, anterodorsal tip slightly projected dorsally, posterodorsal margin separated from hyomandibula outgrowth by small interspace. Hyomandibula long, with well-developed anterior outgrowth; dorsal margin of hyomandibula outgrowth with weak concavity. Opercle long and moderately slender, longer than interopercle. Opercular odontode patch slender, its width about two thirds of dorsal hyomandibula articular facet length. Opercular odontodes 9 or 10, narrow, nearly straight to slightly curved, irregularly arranged. Dorsal process of opercle short, slightly curved, extremity rounded. Opercular articular facet for hyomandibula with rounded lateral shield, articular facet for preopercle small, rounded. Interopercle moderate in length, about three fourths longitudinal length of hyomandibula, with stick-like anterior portion; dorsal process placed near anterior margin of interopercle, anterior socket for ligament connecting interopercle to lower jaw with small anterior projection. Interopercular odontodes 21 or 22, nearly straight, pointed, arranged in irregular longitudinal rows. Preopercle compact, with minute ventral projection. Parurohyal robust, lateral process pointed, slightly curved. Parurohyal head well-developed, with pronounced anterolateral paired process. Middle parurohyal foramen minute. Posterior process of parurohyal moderately long, about three fourths of distance between anterior margin of parurohyal and anterior insertion of posterior process. Branchiostegal rays 8. Vertebrae 40. Ribs 12 or 13. Two dorsal hypural plates corresponding to hypurals 3 + 4 + 5; single ventral hypural plate corresponding to hypurals 1 + 2 + parhypural.

Colouration in alcohol: Dorsal part of flank, dorsum and head side pale brown, ventral part of flank pale brownish yellow, with great concentration of minute, diffuse brown dots, their size about equal or smaller than orbit, sometimes more concentrated and darker along longitudinal midline of flank. Venter and ventral surface of head pale yellow. Barbels pale brown. Fins pale brown to hyaline on extremities.

*Etymology.* The name *listruoides* is an allusion to the superficial similarity of the new species with species of the catfish genus *Listrura* Pinna, 1988 (Trichomycteridae: Microcambevinae), including an elongate body, a rounded caudal fin that is continuous with the caudal peduncle forming a spatula-shaped tail, and an absence of pelvic fin and girdle.

*Distribution.* *Trichomycterus listruoides* is only known from the type locality, the Córrego Tamborete, Rio Grande drainage, upper Rio Paraná basin, at about 875 m asl (Figure 3B).

*Trichomycterus (Cryptocambeva) pirabitira* Barbosa & Azevedo-Santos, 2012  
Figures 6C, 9 and 10A.

*Trichomycterus pirabitira* Barbosa & Azevedo-Santos, 2012: [7] (358) (original description; type locality: Brazil: Estado de Minas Gerais: Município de Conceição da Aparecida: small stream between Carmo do rio Claro and Conceição da Aparecida, a tributary of the rio Grande, rio Paraná basin, approximately 21°8'53'' S, 46°14'95'' W, with altitude approximately 960 m [correctly: stream about 8.5 km SW of Conceição da Aparecida, 21°07'37'' S, 46°16'59'' W, about 965 m asl]; holotype: UFRJ 8335).

*Diagnosis.* *Trichomycterus pirabitira* differs from all other congeners of the subgenus *Cryptocambeva* by the presence of a foramen in the posterior portion of the dorsal process of the interopercle (Figure 6C; vs. foramen absent, Figure 6D). *Trichomycterus pirabitira* is distinguished from other species of *Cryptocambeva*, except for *Trichomycterus claudiae* Barbosa & Costa, 2010, *Trichomycterus mirissumba* Costa, 1992, *Trichomycterus mariamole* Barbosa & Costa, 2010, *Trichomycterus saturatus* Costa, Katz & Azevedo-Santos sp. Nov., and *Trichomycterus vermiculatus* (Eigenmann, 1917), by a combination of the anterior segment of the infraorbital canal being present (vs. absent), seven pectoral-fin rays (vs. six), well-developed pelvic fin and girdle (vs. absent or rudimentary), and three procurrent dorsal-fin rays (vs. two). *Trichomycterus pirabitira* differs from *T. claudiae*, *T. mirissumba*, *T. mariamole*,

and *T. vermiculatus* by having a relatively robust metapterygoid, which is about as long as deep (Figure 6C; vs. slender, deeper than long, Figure 6D); from *T. claudiae*, *T. mirissumba*, and *T. vermiculatus* by having 12–14 ribs (vs. 15 or 16); from *T. claudiae* and *T. vermiculatus* by having the anal-fin origin at vertical through the centrum of the 23rd or 24th vertebra (vs. 25th or 26th); from *T. claudiae* by the absence of a longitudinal black stripe along the midline of the body side (vs. presence); from *T. mirissumba* by having well-delimited spots on the flank (vs. spots diffuse); from *T. vermiculatus* by having 36–38 vertebrae (vs. 39 or 40); and from *T. saturatus* Costa, Katz & Azevedo-Santos sp. Nov. by having flank dots separated by interspaces that are larger than the dots (vs. flank with a great concentration of dark brown dots making the interspace areas smaller than the areas occupied by the dots), an absence of a rounded anterior projection in the interopercle (Figure 6C; vs. presence, Figure 6), a subrectangular basibranchial 3 (Figure 10A; vs. goblet-shaped due to a strong posterior constriction, Figure 10B), and a rudimentary hypobranchial 3 (Figure 10A; vs. well-developed, Figure 10B). For a full description and anatomical illustrations, see Barbosa and Azevedo-Santos [7].



**Figure 9.** *Trichomycterus (Cryptocambeva) pirabitira*, UFRJ 7279, Conceição da Aparecida, 65.7 mm SL: (A) lateral, (B) dorsal, and (C) ventral views.

**Distribution.** Streams at the left margin of the Rio Grande, between the Rio São João and Rio Sapucaí subdrainages, and at altitudes between about 750 and 965 m asl (Figure 3A).

**Material examined.** All specimens from Brazil: Minas Gerais State: Rio Paraná basin, Rio Grande drainage. Conceição da Aparecida Municipality: UFRJ 8335, holotype; UFRJ 8140, six paratypes; UFRJ 8264, three paratypes (C&S); a small stream about 8.5 km SW of Conceição da Aparecida, 21°07'37'' S 46°16'59'' W, at about 965 m asl; V.M. Azevedo-Santos, 30 April 2011.

UFRJ 4927, 11 paratypes; UFRJ 7881, 1 ex. (C&S); a small stream tributary of Córrego Cuiabá, on the way to the village of Nova Resende; D. D'Almeida, M. Gonçalves & M.A. Barbosa, 24 September 1999. UFRJ 7279, 11 paratypes; UFRJ 5829, 3 paratypes (C&S); 7885, 1 ex. (C&S); same locality as UFRJ 4927; J.P.B. Barata, R. Paiva & M.A. Barbosa; 24 September 2006. UFRJ 9914, 7; Córrego Cuiabá, road Conceição da Aparecida-Nova Resende, 21°05'22" S 46°13'43" W, at about 910 m asl; A. M. Katz & P. Bragança, 14 February 2014. Carmo do Rio Claro Municipality: UFRJ 8283, 7; Rio Pedra Molhada, 21°00'23" S 46°15'00" W, at about 855 m asl; V. M. Azevedo-Santos & I. C. Azevedo-Santos, 3 August 2011. UFRJ 12729, 8; Rio Pedra Molhada, 21°00'18" S 46°14'49" W, about 810 m asl; V. M. Azevedo-Santos & A. M. Katz, 30 October 2021. UFRJ 12853, 1; stream tributary of Ribeirão Itaci, 20°55'20" S 45°58'05" W, at about 795 m asl; V. M. Azevedo-Santos & A. M. Katz, 1 November 2021. Fortaleza de Minas Municipality: UFRJ 7273, 47 ex.; UFRJ 7884, 3 ex. (C&S); Riacho Fortaleza, road Jacuí-Fazenda Fortaleza, 20°53'57" S 46°44'09" W, at about 890 m asl; M. A. Barbosa, J. Prata & R. Paiva, 25 September 2006. Capetinga Municipality: UFRJ 8372, 4; stream tributary of Ribeirão Antinha, Rio Grande drainage, Rio Paraná basin, 20°38'23" S 46°59'02" W, at an altitude about 750 m asl; V.M. Azevedo-Santos, 21 August 2011.

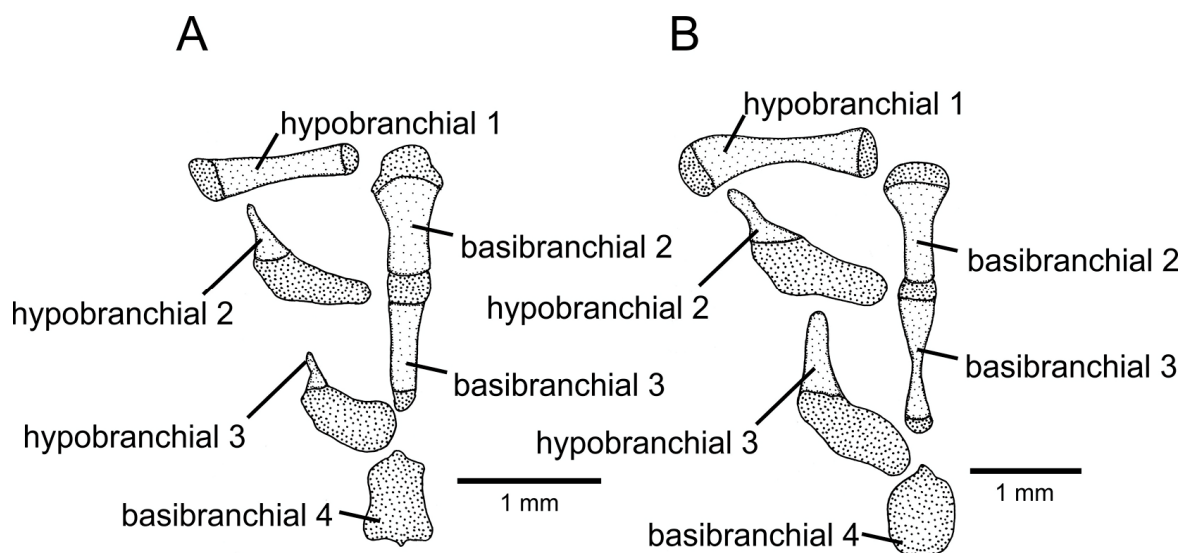


**Figure 10.** Ventral branchial arches, with left-central portion and in dorsal view: (A) *Trichomycterus pirabityra*; (B) *Trichomycterus (Cryptocambeva) saturatus* Costa, Katz & Azevedo-Santos sp. nov. Larger stippling represents cartilage.

*Trichomycterus (Cryptocambeva) saturatus* Costa, Katz & Azevedo-Santos sp. Nov.

LSID: urn:lsid:zoobank.org:act:31E2B7D1-CEEB-43C3-814D-A7F8AF0185CF

Figures 5C, 6E, 7C, 10B and 11; Table 3

**Holotype.** UFRJ 13378, 85.8 mm SL; Brazil: Minas Gerais State: Capitólio Municipality: Córrego Tamborete, a tributary of Rio Grande at the Furnas dam, upper Rio Paraná basin, 20°38'53" S 46°09'55" W, at about 875 m asl; A.M. Katz & P.H.N. Bragança, 14 February 2014.

**Paratypes.** UFRJ 9912, 3 ex., 33.8–59.6 mm SL; UFRJ 13463, 3 ex., 37.1–70.3 mm SL (C&S); CICC AA 07647, 2 ex., 51.5–77.0 mm SL; collected with holotype. UFRJ 12720, 1 ex., 49.3 mm SL; same locality as holotype; V. M. Azevedo-Santos, 13 July 2017. UFRJ 12827, 1 ex., 116.3 mm SL; Córrego Tamborete, 20°38'38" S 46°10'13" W, at about 890 m asl; A. M. Katz & V. M. Azevedo-Santos, 2 November 2021.



**Figure 11.** *Trichomycterus (Cryptocambeva) saturatus* Costa, Katz & Azevedo-Santos sp. nov. Holotype, UFRJ 13378, Capitólio, 85.8 mm SL: (A) lateral, (B) dorsal, and (C) ventral views.

**Diagnosis.** *Trichomycterus saturatus* is distinguished from all other congeners of the subgenus *Cryptocambeva* by having a goblet-shaped basibranchial 3 as a result of a strong posterior constriction (Figure 10B; vs. subrectangular, Figure 10A). *Trichomycterus saturatus* is distinguished from other species of *Cryptocambeva*, except for *T. claudiae*, *T. mirissumba*, *T. mariamole*, *T. pirabitira*, and *T. vermiculatus*, by a combination of an anterior segment of the infraorbital canal being present (vs. absent), seven pectoral-fin rays (vs. six), well-developed pelvic fin and girdle (vs. absent or rudimentary), and three procurrent dorsal-fin rays (vs. two). *Trichomycterus saturatus* differs from *T. claudiae*, *T. mirissumba*, *T. mariamole*, and *T. vermiculatus* by having a relatively robust metapterygoid, which is about as long as deep (Figure 6E; vs. slender, deeper than long, Figure 6D); from *T. claudiae*, *T. mirissumba*, and *T. vermiculatus* by having 14 ribs (vs. 15 or 16); from *T. claudiae* and *T. vermiculatus* by having the anal-fin origin at vertical through the centrum of the 23rd or 24th vertebra (vs. 25th or 26th); from *T. claudiae* by the absence of a longitudinal black stripe along the midline of the body side (vs. presence); from *T. mirissumba* by having well-delimited

spots on the flank (vs. spots diffuse); from *T. pirabitira* by having the flank with a great concentration of dark brown dots making the interspace areas smaller than the areas occupied by the dots (vs. flank dots separated by interspaces that are larger than the dots), the absence of a foramen in the posterior portion of the dorsal process of the interopercle (vs. presence, Figure 6C), the presence of a rounded anterior projection in the interopercle (Figure 6E; vs. absence, Figure 6C), and a well-developed hypobranchial 3 (Figure 10B; vs. rudimentary, Figure 10A).

**Table 3.** Morphometric data of *Trichomycterus saturatus* Costa, Katz & Azevedo-Santos sp. nov.

	Holotype	Paratypes (n = 7)
Standard length (SL)	85.8	40.2–116.3
<b>Percentage of standard length</b>		
Body depth	17.3	8.2–26.7
Caudal peduncle depth	14.3	7.1–22.4
Body width	11.6	5.4–18.3
Caudal peduncle width	3.9	1.9–6.9
Pre-dorsal length	61.9	28.4–86.1
Pre-pelvic length	55.8	28.7–81.1
Dorsal-fin base length	12.5	5.0–18.0
Anal-fin base length	10.6	9.2–14.0
Caudal-fin length	17.7	7.3–23.2
Pectoral-fin length	13.6	5.0–16.0
Pelvic-fin length	10.2	8.9–15.2
Head length	19.9	10.4–27.9
<b>Percentage of head length</b>		
Head depth	60.1	29.2–79.6
Head width	89.9	45.2–123.8
Snout length	43.6	22.5–64.4
Interorbital width	30.3	16.0–42.8
Preorbital length	13.3	5.5–20.3
Eye diameter	9.6	6.0–16.3

*Description.* General morphology: Morphometric data are presented in Table 3. Body relatively deep, subcylindrical anteriorly, compressed posteriorly. Greatest body depth in area immediately anterior to pelvic-fin base. Dorsal and ventral profiles slightly convex between snout and anterior limit of caudal peduncle, nearly straight on caudal peduncle. Anus and urogenital papilla opening at vertical just anterior to middle portion of dorsal-fin base. Head sub-trapezoidal in dorsal view, with anterior profile of snout convex. Eye minute, dorsally positioned on head, nearer snout tip than posterior margin of opercle. Posterior nostril nearer anterior nostril than orbit. Tip of nasal barbel posteriorly reaching opercular patch of odontodes; tip of maxillary and rictal barbels reaching pectoral-fin base. Mouth subterminal. Jaw teeth pointed, irregularly arranged, 51–61 on premaxilla, 36–47 on dentary. Minute skin papillae on dorsal and ventral surfaces of head. Branchial membrane attached to isthmus only at its anterior-most point, in ventral midline.

Dorsal and anal fins subtriangular. Total dorsal-fin rays 11 (ii + II + 7), total anal-fin rays 10 (iii + II + 5). Anal-fin origin at vertical through posterior portion of dorsal-fin base, at vertical through base of 5<sup>th</sup> bifid dorsal-fin ray. Dorsal-fin origin at vertical through centrum of 19th or 20th vertebra; anal-fin origin at vertical through centrum of 23rd or 24th vertebra. Pectoral fin subtriangular in dorsal view, first pectoral-fin ray terminating in filament about 25–40 % pectoral-fin length excluding filament. Total pectoral-fin rays 7 (I + 6). Pelvic fin subtruncate, posteriorly overlapping anus and urogenital papilla, its posterior extremity at vertical just posterior to middle portion of dorsal-fin base. Pelvic-fin

bases medially separated by minute interspace. Total pelvic-fin rays 5 (I + 4). Caudal fin truncate, posterior corners slightly rounded. Total principal caudal-fin rays 13 (I + 11 + I), total dorsal procurrent rays 21 (xx + I), total ventral procurrent rays 16 or 17 (xv–xvi + I).

Laterosensory system: Supraorbital, posterior section of infraorbital canal and postorbital canal continuous. Supraorbital sensory canal pores 3: s1, adjacent to medial margin of anterior nostril; s3, adjacent and just posterior to medial margin of posterior nostril; s6, in transverse line through posterior half of orbit; pore s6 slightly nearer its homologous pore than orbit. Infraorbital sensory canal arranged in 2 segments; anterior section isolated, with two pores: i1, at transverse line through anterior nostril, i3, at transverse line just anterior to posterior nostril; posterior segment posteriorly connected to supraorbital and postorbital canal, with 2 pores: i10, adjacent to ventral margin of orbit, i11, posterior to orbit. Postorbital canal pores 2: po1, at vertical through posterior portion of interopercular patch of odontodes, and po2, at vertical through posterior portion of opercular patch of odontodes. Lateral line pores 2; posterior-most pore at vertical just posterior to pectoral-fin base.

Osteology: Mesethmoid slender, anterior margin straight to slightly concave, main axis gradually widening posteriorly. Mesethmoid cornu narrow, tip rounded. Postero-lateral margin of lateral ethmoid with small projection. Antorbital thin, sub-elliptical, separated from sesamoid supraorbital by interspace shorter than antorbital length. Sesamoid supraorbital slender, without lateral projections, its length about two times antorbital length. Premaxilla sub-trapezoidal in dorsal view, laterally tapering, longer than maxilla. Maxilla slightly curved. Autopalatine sub-rectangular in dorsal view when excluding its postero-lateral process, its largest width about half its length including anterior cartilage; medial margin weakly concave. Autopalatine posterolateral process well-developed, its length slightly larger than autopalatine largest width. Metapterygoid subtriangular, deeper than long, dorsal extremity rounded, anterior margin convex, continuous, posterior portion without distinctive projection. Quadrate compact, dorsal margin with weak projection posterior to articulation to metapterygoid, posterodorsal margin separated from hyomandibula outgrowth by minute interspace. Hyomandibula long, with well-developed anterior outgrowth; dorsal margin of hyomandibula outgrowth with small concavity on its posterior portion. Opercle long and slender, slightly longer than interopercle. Opercular odontode patch slender, its width about one third of dorsal hyomandibula articular facet. Opercular odontodes 10–13, narrow, nearly straight, arranged in irregular oblique rows. Dorsal process of opercle short, slightly curved, extremity pointed. Opercular articular facet for hyomandibula with rounded lateral shield, articular facet for preopercle rudimentary, rounded. Interopercle moderate in length, about three fourths longitudinal length of hyomandibula, with rounded anterior projection; dorsal process posteriorly placed to anterior margin of interopercle. Interopercular odontodes 36 or 39, nearly straight, pointed, arranged in irregular longitudinal rows. Preopercle compact, with minute ventral projection. Basibranchial 2 robust, anterior portion slightly wider; basibranchial 3 goblet-shaped, with posterior constriction. Hypobranchial ossifications well-developed. Parurohyal robust, lateral process pointed, slightly curved. Parurohyal head well-developed, with almost indistinct anterolateral paired process. Middle parurohyal foramen small, rounded. Posterior process of parurohyal moderately long, about three fourths of distance between anterior margin of parurohyal and anterior insertion of posterior process. Branchiostegal rays 8 or 9. Vertebrae 37–39. Ribs 14. One or two dorsal hypural plates corresponding to hypurals 3 + 4 + 5; single ventral hypural plate corresponding to hypurals 1 + 2 + parhypural.

Colouration in alcohol: Flank with great concentration of dark brown dots over pale brownish yellow ground, making areas without dots smaller than areas occupied by dots; dots darker on dorsal portion of flank. Dorsum and dorsal surface of head brown with dots slightly darker than colour ground, venter and ventral surface of head light yellow. Barbels brown. Fins hyaline with brown dots on basal portion; brown chromatophores concentrate along rays of pectoral and unpaired fins. Smallest specimen (33.1 mm SL), with dots darker and highly coalesced along median longitudinal line of flank; dots smaller and more concentrated on dorsal portion of flank.

*Etymology.* From the Latin word *saturatus* (=saturated), its name is an allusion to the colour pattern consisting of numerous dark brown dots concentrated over the whole flank, making the interspaces smaller than the areas occupied by overlapped dots.

*Distribution.* *Trichomycterus saturatus* is only known from its type locality, the Córrego Tamborete, Rio Grande drainage, Rio Paraná basin, at about 875 m asl (Figure 3B).

*Remarks.* An examination of the gut content of the largest (70.3 mm SL) cleared and stained paratype (UFRJ 13463) revealed the presence of a chironomid larva, an unidentified insect larva, and a juvenile (about 20 mm SL) of *Phalloceros* sp. (Cypridontiformes: Poeciliidae), consisting of the first record of ichthyophagy in eastern South American trichomycterines.

*Trichomycterus (Cryptocambeva) uberabensis* Costa, Azevedo-Santos & Katz sp. nov.

LSID: urn:lsid:zoobank.org:act: CADF9135-EEEE-4E46-A124-90F99B70EA3C

Figures 5D, 6F, 7D and 12; Table 4

*Holotype.* UFRJ 13366, 42.3 mm SL; Brazil: Minas Gerais State: Veríssimo Municipality: stream tributary of Rio Uberaba, Rio Grande drainage, upper Rio Paraná basin, 19°39'21" S 48°15'21" W, at about 665 m asl; V.M. Azevedo-Santos et al., 15 April 2022.

*Paratypes.* UFRJ 12921, 8 ex., 23.3–39.9 mm SL; UFRJ 12957, 3 ex., 31.3–40.3 mm SL (C&S); CICCAA 07648, 2 ex., 31.9–32.7 mm SL; UFRJ 12894, 4 ex., 12.2–26.0 mm SL (DNA); collected with holotype.

*Diagnosis.* *Trichomycterus uberabensis* differs from all other congeners of *Cryptocambeva*, except for *T. candidus* and *T. listruoides*, by the absence of pelvic fin and girdle (vs. presence). *Trichomycterus uberabensis* is distinguished from *T. candidus* and *T. listruoides* by having fewer ventral procurrent caudal-fin rays (13–16 vs. 20), more teeth on the dentary (29–32 vs. 21–25), and a unique colour pattern on the flank, comprising small dark brown to black spots that are larger than the orbital diameter (vs. minute dark brown dots equal to or smaller than the orbital diameter in *T. candidus*, and small vermiculate marks in *T. listruoides*). *Trichomycterus uberabensis* also differs from *T. listruoides* by having the caudal-fin margin not aligned with the caudal peduncle, which is not dorsally expanded (vs. in a continuous line, with the dorsal margin of the caudal peduncle being slightly expanded), fewer dorsal procurrent caudal-fin rays (17–19 vs. 24 or 25), fewer vertebrae (37 or 38 vs. 40), the dorsal-fin origin at vertical through the centrum of the 22nd vertebra (vs. 24th), and the anal-fin origin at vertical through the centrum of the 24th or 25th vertebra (vs. 26th or 27th). It differs from *T. candidus* by having more interopercular odontodes (21–24 vs. 16–19).

*Description.* General morphology: Morphometric data are presented in Table 4. Body slender, subcylindrical anteriorly, compressed posteriorly. Greatest body depth in area approximately at midway between pectoral-fin base and vertical through dorsal-fin origin. Dorsal and ventral profiles slightly convex between snout and anterior limit of caudal peduncle, about straight on caudal peduncle. Anus and urogenital papilla opening at vertical just posterior of dorsal-fin origin. Head sub-trapezoidal in dorsal view, with anterior profile of snout convex. Eye small, dorsally positioned on head, nearer snout tip than posterior margin of opercle. Posterior nostril nearer anterior nostril than orbit. Tip of nasal barbel posteriorly reaching between middle of opercle or area immediately posterior to it; tip of maxillary barbel reaching area between interopercle and pectoral-fin base, sometimes reaching pectoral-fin base; rictal barbel reaching between posterior portion of interopercular patch of odontodes and area between interopercle and pectoral-fin base. Mouth subterminal. Jaw teeth pointed, irregularly arranged, 26–28 on premaxilla, 29–32 on dentary. Minute skin papillae on dorsal and ventral surfaces of head. Branchial membrane attached to isthmus only at its anterior-most point, in ventral midline.



**Figure 12.** *Trichomycterus (Cryptocambeva) uberabensis* Costa, Azevedo-Santos & Katz sp. nov. Holotype, UFRJ 13366, Veríssimo, 42.3 mm SL: (A) lateral, (B) dorsal, and (C) ventral views.

Dorsal and anal fins slender, margin slightly convex. Total dorsal-fin rays 11 (ii + II + 7), total anal-fin rays 9 (ii + II + 5). Anal-fin origin at vertical through anterior half of dorsal-fin base, at vertical through base of 2nd or 3rd branched dorsal-fin ray. Dorsal-fin origin at vertical through centrum of 22nd vertebra; anal-fin origin at vertical between centrum of 24th or 25th vertebra. Pectoral fin subtriangular in dorsal view, first pectoral-fin ray terminating in short filament about 10–20 % pectoral-fin length excluding filament. Total pectoral-fin rays 6 (I + 5). Pelvic fin and girdle absent. Caudal fin rounded, nearly continuous with caudal peduncle. Total principal caudal-fin rays 13 (I + 11 + I), total dorsal procurrent rays 17–19 (xvi–xviii + I), total ventral procurrent rays 13–16 (xii–xv + I).

Laterosensory system: Supraorbital, posterior section of infraorbital canal and postorbital canal continuous. Supraorbital sensory canal pores 3: s1, adjacent to medial margin of anterior nostril; s3, adjacent and just posterior to medial margin of posterior nostril; s6, in transverse line through posterior half of orbit; pore s6 nearer adjacent orbit than its homologous pore pair. Anterior infraorbital sensory canal absent. Posterior infraorbital sensory canal pores 2: pore i10, adjacent to ventral margin of orbit, and pore i11, posterior to orbit. Postorbital canal pores 2: po1, at vertical through posterior portion of interopercular patch of odontodes, and po2, at vertical through posterior portion of opercular patch of odontodes. Lateral line pores 2; posterior-most pore at vertical just posterior to pectoral-fin base.

**Table 4.** Morphometric data of *Trichomycterus uberabensis* Costa, Azevedo-Santos & Katz sp. nov.

	Holotype	Paratypes ( <i>n</i> = 8)
Standard length (SL)	60.8	31.3–40.3
<b>Percentage of standard length</b>		
Body depth	14.9	12.1–14.6
Caudal peduncle depth	12.7	9.3–12.2
Body width	9.8	7.3–10.2
Caudal peduncle width	5.0	2.5–4.2
Pre-dorsal length	66.7	49.6–63.1
Dorsal-fin base length	11.5	8.4–11.2
Anal-fin base length	9.3	7.3–9.6
Caudal-fin length	19.1	14.4–18.7
Pectoral-fin length	11.8	9.3–12.4
Head length	17.7	14.0–17.7
<b>Percentage of head length</b>		
Head depth	53.3	49.7–55.1
Head width	84.1	77.2–87.0
Snout length	41.0	38.2–40.9
Interorbital width	23.0	19.3–26.7
Preorbital length	10.0	7.4–10.4
Eye diameter	11.6	8.6–18.9

Osteology: Mesethmoid slender, anterior margin slightly concave, main axis abruptly widening posteriorly. Mesethmoid cornu narrow, tip rounded. Postero-lateral margin of lateral ethmoid with inconspicuous projection. Antorbital thin, small, drop-shaped, separated from sesamoid supraorbital by interspace larger than antorbital length. Sesamoid supraorbital slender, without lateral projections, its length about three times antorbital length. Premaxilla sub-trapezoidal in dorsal view, laterally tapering, shorter than maxilla. Maxilla slightly curved. Autopalatine sub-rectangular in dorsal view when excluding its postero-lateral process, its largest width about half its length including anterior cartilage; medial margin concave. Autopalatine posterolateral process well-developed, its length slightly larger than autopalatine largest width. Metapterygoid subtriangular, deeper than long, dorsal extremity slightly pointed, anterior margin convex, posterior margin with concavity, posterior portion with distinctive posterior projection. Quadrate compact, dorsal margin with weak projection posterior to articulation to metapterygoid, anterodorsal tip slightly projected dorsally, posterodorsal margin separated from hyomandibula outgrowth by small interspace. Hyomandibula long, with well-developed anterior outgrowth; dorsal margin of hyomandibula outgrowth with weak concavity. Opercle long and moderately slender, longer than interopercle. Opercular odontode patch slender, its width about half length of dorsal hyomandibula articular facet. Opercular odontodes 8 or 9, narrow, nearly straight to slightly curved, irregularly arranged. Dorsal process of opercle short, slightly curved, extremity pointed. Opercular articular facet for hyomandibula with rounded lateral shield, articular facet for preopercle minute, rounded. Interopercle moderate in length, about three fourths longitudinal length of hyomandibula, with broad, rounded anterior portion; dorsal process placed near anterior margin of interopercle, anterior socket for ligament connecting interopercle to lower jaw with small anterior projection. Interopercular odontodes 21–24, nearly straight, pointed, arranged in irregular longitudinal rows. Preopercle compact, with small ventral projection. Parurohyal robust, lateral process pointed, nearly straight. Parurohyal head well-developed, with pronounced anterolateral paired process. Middle parurohyal foramen small, rounded. Posterior process of parurohyal moderately long, about four fifths of distance between anterior margin of parurohyal and

anterior insertion of posterior process. Branchiostegal rays 7 or 8. Vertebrae 37 or 38. Ribs 11 or 12. Two dorsal hypural plates corresponding to hypurals 3 + 4 + 5; single ventral hypural plate corresponding to hypurals 1 + 2 + parhypural.

Colouration in alcohol: Flank, dorsum and head side brownish grey, with black dots, about equal or slightly larger than orbital diameter, sometimes coalesced on lateral midline of trunk. Venter and ventral surface of head white. Barbels pale brown. Fins hyaline, with dark brown dots on basal region.

*Etymology.* The name *uberabensis* is a reference to the occurrence of this new species in the Rio Uberaba drainage.

*Distribution.* *Trichomycterus uberabensis* is only known from its type locality, a stream tributary of Rio Uberaba, Rio Grande drainage, upper Rio Paraná basin, at about 665 m asl (Figure 3B).

### 3.2.2. Subgenus *Paracambeva* Costa, 2021

Species of *Paracambeva* are easily distinguished from species of other subgenera of *Trichomycterus* by the presence of a continuous, broad dark grey to black stripe between the snout and the caudal-fin base. All species of *Paracambeva* occurring in the upper Rio Paraná basin are members of a clade named *T. reinhardti* species group Costa & Katz, 2021, which are readily diagnosable by their infraorbital canal not being attached to the antorbital (Costa, 2021). Species of this group are commonly found in small shallow streams, being collected under marginal plants or in gravel substrates.

*Trichomycterus (Paracambeva) adautoleitei* Costa, Azevedo-Santos & Katz sp. nov.

LSID: urn:lsid:zoobank.org:act:07AF9548-552D-4DD7-8964-2A611CD8A70C

Figures 5E, 6G, 7E and 13; Table 5

*Trichomycterus septemradiatus* non *Trichomycterus septemradiatus* Katz, Barbosa & Costa, 2013: [5] (5) in part (misidentification); [11] (337) (misidentification).

*Holotype.* UFRJ 13406, 57.1 mm SL; Brazil: Minas Gerais State: Carmo do Rio Claro Municipality: stream tributary of Rio Itaci, a tributary of Rio Sapucaí, Rio Grande drainage, upper Rio Paraná basin, 20°54'58" S 45°56'21" W, at about 840 m asl; A. M. Katz & V.M. Azevedo-Santos, 31 October 2021.

*Paratypes.* UFRJ 13407, 3 ex., 33.9–50.2 mm SL; collected with holotype. UFRJ 13408, 2 ex., 46.2–49.0 mm SL (C&S); CICCAA 07649, 2 ex., 37.9–46.9 mm SL; same locality as holotype; V.M. Azevedo-Santos, 6 July 2021. UFRJ 13409, 6 ex., 24.5–56.5 mm SL; same locality as holotype; V.M. Azevedo-Santos, 14 July 2021.

*Diagnosis.* *Trichomycterus adautoleitei* differs from all other congeners of *Paracambeva* by having a long pectoral-fin filament, with its length about 40% of the pectoral-fin length excluding the filament (vs. about 20% or less), and some aspects of the colour pattern, including the presence of round black spots on the dorsum (vs. absence in all other species), the absence of a longitudinal series of dark brown to black dots on the dorsal part of the flank (vs. presence in all other species), and a longitudinal midline stripe that is well delimited, black, and highly contrasting with the yellow ground of the flank (vs. with diffuse margins and not highly contrasting with the colour ground of the flank in all other species, except for *T. reinhardti* (Eigenmann, 1917)). *Trichomycterus adautoleitei* is also distinguished from all other species of *Paracambeva*, except for *Trichomycterus funebris* Katz & Costa, 2021, *Trichomycterus ingaiensis* Katz & Costa, 2021, and *Trichomycterus septemradiatus* Katz, Barbosa & Costa, 2013, by having seven pectoral-fin rays (vs. six). *Trichomycterus adautoleitei* differs from *T. ingaiensis* and *T. septemradiatus* by having more ventral procurrent caudal-fin rays (13 vs. 8–11), and from *T. funebris* by having fewer vertebrae (35 or 36 vs. 37 or 38), the dorsal-fin origin at vertical through the centrum of the 19th or 20th vertebra (vs. 22nd), and the anal-fin origin at vertical through the centrum of the 22nd or 23rd vertebra (vs. 25th or 26th).



**Figure 13.** *Trichomycterus (Paracambeva) adautoleitei* Costa, Azevedo-Santos & Katz sp. nov. Holotype, UFRJ 13406, Carmo do Rio Claro, 57.1 mm SL: (A) lateral, (B) dorsal, and (C) ventral views.

*Description.* General morphology: Morphometric data presented in Table 5. Body relatively slender, subcylindrical on anterior region, compressed on posterior region. Greatest body depth in area immediately anterior to pelvic-fin base. Dorsal and ventral profiles slightly convex between snout and dorsal-fin base end, nearly straight on caudal peduncle. Anus and urogenital papilla opening at vertical just posterior to dorsal-fin base. Head sub-trapezoidal, with anterior profile of snout slightly convex in dorsal view. Eye small, dorsally positioned on head, nearer snout tip than posterior margin of opercle. Posterior nostril slightly nearer anterior nostril than orbital rim. Tip of nasal barbel posteriorly reaching opercular patch of odontodes, tip of maxillary barbel reaching pectoral-fin base, and tip of rictal barbel reaching area just posterior to interopercular patch of odontodes. Mouth subterminal. Jaw teeth pointed, irregularly arranged, 39–41 on premaxilla, 40–43 on dentary. Minute skin papillae on dorsal and ventral surfaces of head. Branchial membrane attached to isthmus only at its anterior-most point, in ventral midline.

**Table 5.** Morphometric data of *Trichomycterus adautoleitei* Costa, Azevedo-Santos & Katz sp. nov.

	Holotype	Paratypes ( <i>n</i> = 5)
Standard length (SL)	57.1	43.3–56.5
<b>Percentage of standard length</b>		
Body depth	15.3	11.5–17.1
Caudal peduncle depth	11.7	9.0–11.8
Body width	11.6	7.2–9.7
Caudal peduncle width	4.5	2.0–4.1
Pre-dorsal length	65.0	52.9–58.5
Pre-pelvic length	60.6	48.0–61.8
Dorsal-fin base length	10.1	8.8–10.0
Anal-fin base length	8.0	7.3–8.2
Caudal-fin length	15.6	14.6–16.8
Pectoral-fin length	11.9	10.4–13.1
Pelvic-fin length	8.0	6.0–8.3
Head length	18.4	15.2–18.1
<b>Percentage of head length</b>		
Head depth	49.5	37.7–49.5
Head width	84.8	65.2–84.8
Snout length	42.8	34.1–42.8
Interorbital width	28.3	22.5–28.3
Preorbital length	8.7	8.7–9.8
Eye diameter	10.8	8.3–11.5

Dorsal and anal fins subtriangular. Total dorsal-fin rays 10 or 11 (ii + I–II + 7), total anal-fin rays 9 (ii + II + 5). Anal-fin origin at vertical just posterior to middle of dorsal-fin base, between base of 3rd and 4th branched dorsal-fin rays. Dorsal-fin origin at vertical through centrum of 19th or 20th vertebra; anal-fin origin at vertical through centrum of 22nd or 23rd vertebra. Pectoral fin subtriangular in dorsal view, first pectoral-fin ray terminating in filament about 40% of pectoral-fin length excluding filament. Total pectoral-fin rays 7 (I + 6). Pelvic fin rounded, its posterior extremity at vertical slightly posterior to dorsal-fin origin. Pelvic-fin bases medially separated by minute interspace. Total pelvic-fin rays 5 (I + 4). Caudal fin subtruncate, posterior corners rounded. Total principal caudal-fin rays 13 (I + 11 + I), total dorsal procurrent rays 16 (xv + I), total ventral procurrent rays 13 (ix–x + I).

Laterosensory system: Supraorbital, posterior section of infraorbital canal and postorbital canal continuous. Supraorbital sensory canal pores 3: s1, adjacent to medial margin of anterior nostril; s3, adjacent and just posterior to medial margin of posterior nostril; s6, in transverse line through posterior half of orbit; pore s6 nearer orbit than its homologous pore. Infraorbital sensory canal arranged in 2 segments; anterior section isolated, with two pores: i1, at transverse line through anterior nostril, i3, at transverse line just anterior to posterior nostril; posterior segment posteriorly connected to supraorbital and postorbital canal, with 2 pores: i10, adjacent to ventral margin of orbit, i11, posterior to orbit. Postorbital canal pores 2: po1, at vertical through posterior portion of interopercular patch of odontodes, and po2, at vertical through posterior portion of opercular patch of odontodes. Lateral line pores 2; posterior-most pore at vertical just posterior to pectoral-fin base.

Osteology: Mesethmoid slender, anterior margin approximately straight, main axis gradually widening posteriorly. Mesethmoid cornu narrow, tip rounded. Postero-lateral margin of lateral ethmoid without projections. Antorbital slender, thin, drop-shaped, separated from sesamoid supraorbital by interspace larger than antorbital length. Sesamoid supraorbital slender, without lateral projections, its length about two and half times antorbital length. Premaxilla sub-trapezoidal in dorsal view, laterally tapering, slightly

longer than maxilla. Maxilla slightly curved. Autopalatine sub-rectangular in dorsal view when excluding its postero-lateral process, its largest width about half its length including anterior cartilage; medial margin weakly concave. Autopalatine posterolateral process well-developed, its length about half autopalatine length excluding anterior cartilage. Metapterygoid subtrapezoidal, about so deep as long, dorsal extremity truncate, anterior margin slightly convex, posterior margin slightly concave, posterior portion with small posterior projection. Quadrate compact, dorsal margin with weak projection posterior to articulation to metapterygoid, posterodorsal margin separated from hyomandibula outgrowth. Hyomandibula long, with well-developed anterior outgrowth; dorsal margin of hyomandibula outgrowth with deep concavity. Opercle long and moderately slender, longer than interopercle. Opercular odontode patch slender, its width about three fifths of dorsal hyomandibula articular facet. Opercular odontodes 13–15, narrow, about straight, irregularly arranged. Dorsal process of opercle short, slightly curved, dorsally terminating in stick-like tip. Opercular articular facet for hyomandibula with rounded lateral shield, articular facet for preopercle small, rounded. Interopercle moderate in length, about three fourths longitudinal length of hyomandibula, with convex anterior portion; dorsal process placed near anterior margin of interopercle. Interopercular odontodes 33–35, nearly straight, tip pointed to slightly rounded, arranged in irregular longitudinal rows. Preopercle compact, with minute ventral projection. Parurohyal robust, lateral process pointed, nearly straight. Parurohyal head well-developed, with pronounced anterolateral paired process. Middle parurohyal foramen minute. Posterior process of parurohyal short, about half distance between anterior margin of parurohyal and anterior insertion of posterior process. Branchiostegal rays 8. Vertebrae 35 or 36. Ribs 15. Two dorsal hypural plates corresponding to hypurals 3 + 4 + 5; single ventral hypural plate corresponding to hypurals 1 + 2 + parhypural.

Colouration in alcohol: Flank, dorsum and head side dark yellow, to slightly lighter on ventral part of flank, with black dots on dorsum, black stripe along longitudinal midline of flank, and sometimes few black dots on posterior portion of caudal peduncle. Dark chromatophores concentrated on area between maxillary barbel and longitudinal flank stripe, on area between middle portion of dorsal surface of head and nape, and in oblique zone anterior to opercular and interopercular patches of odontodes; black dots on snout and barbels. Venter and ventral surface of head light yellow. Fins hyaline, with minute black dots on whole dorsal and caudal fins, and on first pectoral-fin ray, and diffuse grey stripe on caudal fin longitudinal midline.

*Etymology.* It is named in honour of Antônio Aduino Leite (1927–2020), the founder of the Museum of Indigenous Archaeology of Carmo do Rio Claro (MUARI), which has a rich collection of archaeological pieces between 2000 and 12,000 years old, mainly found in the region of the type locality of the new species.

*Distribution.* *Trichomycterus adautoleitei* is only known from its type locality, a stream tributary of Rio Itaci, a tributary of Rio Sapucaí, Rio Grande drainage, upper Rio Paraná basin, at about 840 m asl (Figure 3C).

*Trichomycterus (Paracambeva) coelhorum* Costa, Azevedo-Santos & Katz sp. nov.

LSID: urn:lsid:zoobank.org:act:6BCFCCC8-60AE-423D-8EF2-189469BFBE0E

Figures 5F, 6H, 7F and 14; Table 6



**Figure 14.** *Trichomycterus (Paracambeva) coelhorum* Costa, Azevedo-Santos & Katz sp. nov. Holotype, UFRJ 13410, Veríssimo, 44.8 mm SL: (A) lateral, (B) dorsal, and (C) ventral views.

*Holotype.* UFRJ 13410, 44.8 mm SL; Brazil: Minas Gerais State: Veríssimo Municipality: stream tributary of Rio Uberaba, Rio Grande drainage, upper Rio Paraná basin, 19°39'21" S 48°15'21" W, at about 665 m asl; V. M. de Azevedo Santos et al., 15 April 2022.

*Paratypes.* UFRJ 12916, 5 ex., 30.7–39.3 mm SL; UFRJ 12961, 3 ex., 34.9–38.8 mm SL (C&S); CICCAA 07650, 4 ex., 32.2–36.8 mm SL; collected with holotype.

*Diagnosis.* *Trichomycterus coelhorum* is distinguished from all other congeners of *Paracambeva* by having fewer dorsal procurent caudal-fin rays (10–12 vs. 13–25). *Trichomycterus coelhorum* is also distinguished from all other congeners of *Paracambeva*, except for *T. humboldti* Costa & Katz, 2021, *Trichomycterus pauciradiatus* Alencar & Costa, 2006, *Trichomycterus piratymbara* Katz, Barbosa & Costa, 2013, *T. reinhardti*, and *T. sainthilairei*, by having six pectoral-fin rays. *Trichomycterus coelhorum* differs from *T. humboldti*, *T. pauciradiatus*, *T. piratymbara*, *T. reinhardti*, and *T. sainthilairei* by having fewer ventral procurent caudal-fin rays (9 or 10 vs. 11–18); from *T. piratymbara*, *T. reinhardti*, and *T. sainthilairei* by having fewer vertebrae (34–36 vs. 37–40); from *T. piratymbara*, *T. humboldti*, and *T. pauciradiatus* by having fewer ribs (12–14 vs. 15–19); and from *T. humboldti* and *T. pauciradiatus* by having five pelvic-fin rays (vs. four).

**Table 6.** Morphometric data of *Trichomycterus coelhorum* Costa, Azevedo-Santos & Katz sp. nov.

	Holotype	Paratypes (n = 10)
Standard length (SL)	60.8	34.4–38.8
<b>Percentage of standard length</b>		
Body depth	15.2	11.1–15.1
Caudal peduncle depth	10.6	8.7–10.2
Body width	9.4	7.6–9.9
Caudal peduncle width	3.6	2.5–3.5
Pre-dorsal length	62.6	51.5–59.7
Pre-pelvic length	61.7	47.5–54.3
Dorsal-fin base length	11.7	8.5–11.2
Anal-fin base length	7.8	6.7–8.3
Caudal-fin length	17.3	13.4–19.9
Pectoral-fin length	11.4	9.0–12.2
Pelvic-fin length	8.4	6.7–8.0
Head length	18.8	15.0–17.0
<b>Percentage of head length</b>		
Head depth	52.3	42.8–51.1
Head width	81.2	66.5–76.0
Snout length	39.2	30.9–38.0
Interorbital width	27.6	22.6–24.9
Preorbital length	8.3	7.1–10.7
Eye diameter	11.9	8.3–10.7

*Description.* General morphology: Morphometric data are presented in Table 6. Body relatively deep, subcylindrical anteriorly, compressed posteriorly. Greatest body depth in area immediately anterior to pelvic-fin base. Dorsal and ventral profiles slightly convex between snout and anterior limit of caudal peduncle, nearly straight on caudal peduncle. Anus and urogenital papilla opening at vertical through anterior third of dorsal-fin base. Head sub-trapezoidal in dorsal view, with anterior profile of snout convex. Eye minute, dorsally positioned on head, nearer snout tip than posterior margin of opercle. Posterior nostril nearer anterior nostril than orbit. Tip of nasal barbel posteriorly reaching opercular patch of odontodes or area just anterior to it; tip of maxillary barbel reaching between posterior portion of interopercular patch of odontodes and pectoral-fin base; rictal barbel reaching between middle and posterior portions of interopercular patch of odontodes. Mouth subterminal. Jaw teeth pointed, irregularly arranged, 30–34 on premaxilla, 29–31 on dentary. Minute skin papillae on dorsal and ventral surfaces of head. Branchial membrane attached to isthmus only at its anterior-most point, in ventral midline.

Dorsal and anal fins subtriangular. Total dorsal-fin rays 11 (ii + II–III + 5–6 + I), total anal-fin rays 9 (ii + II + 4 + I). Anal-fin origin at vertical through middle portion of dorsal-fin base, at vertical through base of 5th or 6th segmented dorsal-fin ray. Dorsal-fin origin at vertical through centrum of 19th or 20th vertebra; anal-fin origin at vertical through centrum of 19th or 20th vertebra. Pectoral fin subtriangular in dorsal view, first pectoral-fin ray terminating in minute filament about 5–10 % of pectoral-fin length excluding filament. Total pectoral-fin rays 6 (I + 5). Pelvic fin rounded, posteriorly overlapping anus but not reaching urogenital papilla, its posterior extremity at vertical through base of first bifid dorsal-fin ray. Pelvic-fin bases medially separated by minute interspace. Total pelvic-fin rays 5 (I + 4). Caudal fin subtruncate, posterior corners rounded. Total principal caudal-fin rays 13 (I + 11 + I), total dorsal procurrent rays 10 – 12 (ix–xi + I), total ventral procurrent rays 9 or 10 (viii–ix + I).

Laterosensory system: Supraorbital, posterior section of infraorbital canal and postorbital canal continuous. Supraorbital sensory canal pores 3: s1, adjacent to medial margin of anterior nostril; s3, adjacent and just posterior to medial margin of posterior nostril; s6, in transverse line through posterior half of orbit; pore s6 nearer orbit than its homologous pore. Infraorbital sensory canal arranged in 2 segments; anterior section isolated, with two pores: i1, at transverse line through anterior nostril, i3, at transverse line just anterior to posterior

nostril; posterior segment posteriorly connected to supraorbital and postorbital canal, with 2 pores: i10, adjacent to ventral margin of orbit, i11, posterior to orbit. Postorbital canal pores 2: po1, at vertical through posterior portion of interopercular patch of odontodes, and po2, at vertical through posterior portion of opercular patch of odontodes. Lateral line pores 2; posterior-most pore at vertical just posterior to pectoral-fin base.

Osteology: Mesethmoid slender, anterior margin approximately straight, main axis gradually widening posteriorly. Mesethmoid cornu narrow, tip rounded. Postero-lateral margin of lateral ethmoid without projections. Antorbital thin, drop-shaped, separated from sesamoid supraorbital by interspace larger than antorbital length. Sesamoid supraorbital slender, without lateral projections, short, its length about two times antorbital length. Premaxilla sub-trapezoidal in dorsal view, slightly longer than maxilla. Maxilla slightly curved. Autopalatine sub-rectangular in dorsal view when excluding its postero-lateral process, its largest width about three fourths of its length including anterior cartilage; medial margin weakly concave. Autopalatine posterolateral process well-developed, its length about equal autopalatine largest width. Metapterygoid subtriangular, deeper than long, dorsal extremity pointed, anterior convex, posterior margin concave, posterior portion with small posterior projection. Quadrate compact, dorsal margin with weak projection posterior to articulation to metapterygoid, posterodorsal margin in contact with hyomandibula outgrowth. Hyomandibula long, with well-developed anterior outgrowth; dorsal margin of hyomandibula gently concave. Opercle long and moderately slender, longer than interopercle. Opercular odontode patch slender, its width about three fifths of dorsal hyomandibula articular facet. Opercular odontodes 18–20, narrow, about straight, irregularly arranged. Dorsal process of opercle short, subtriangular. Opercular articular facet for hyomandibula with rounded lateral shield, articular facet for preopercle small, rounded. Interopercle short, about half longitudinal length of hyomandibula, with convex anterior portion; dorsal process placed nearly continuous with anterior margin of interopercle. Interopercular odontodes 26–28, nearly straight, tip pointed, arranged in irregular longitudinal rows. Preopercle compact, with minute ventral projection. Parurohyal robust, lateral process pointed, nearly straight to slightly curved. Parurohyal head well-developed, with pronounced anterolateral paired process. Middle parurohyal foramen large, elliptical. Posterior process of parurohyal short, about half distance between anterior margin of parurohyal and anterior insertion of posterior process. Branchiostegal rays 8. Vertebrae 35 or 36. Ribs 15. Two dorsal hypural plates corresponding to hypurals 3 + 4 + 5; single ventral hypural plate corresponding to hypurals 1 + 2 + parhypural.

Colouration in alcohol: Flank pale yellow, with dark brown to black stripe along longitudinal midline of flank and black dots above stripe, more concentrated on caudal peduncle; often faint minute brown dots on ventral portion of caudal peduncle side and above venter. Dorsum pale brown, with two longitudinal dark brown to black stripes and minute black dots between stripes. Lateral and dorsal surfaces of head pale yellow with brown dots. Venter and ventral surface of head yellowish white. Barbels brown. Fins hyaline, with minute black dots on whole dorsal and caudal fins, and on first pectoral-fin ray; diffuse grey stripe on caudal fin longitudinal midline.

*Etymology.* The name *coelhorum* is in honour of the Coelho family from Frutal Municipality in Minas Gerais State. This is in recognition of the help of the zoologist Paula Nunes Coelho with the type series and her family for the logistical support during studies in the region.

*Distribution.* *Trichomycterus coelhorum* is only known from its type locality, a stream tributary of the Rio Uberaba, Rio Grande drainage, upper Rio Paraná basin, at about 665 m asl (Figure 3C).

*Trichomycterus (Paracambeva) saintthilairei* Katz & Costa, 2021

Figure 14

*Trichomycterus piratymbara* non *Trichomycterus piratymbara* Katz & Costa, 2013: [42] (238) (misidentification).

*Trichomycterus sainthilairei* Katz & Costa, 2021: [1] (17) (original description; type locality: Brazil: Estado de Minas Gerais: Município de Capitólio: Córrego Tamborete, Rio Grande drainage, Rio Paraná basin, 20°38'53" S 46°09'55" W, at an altitude about 875 m asl; holotype: UFRJ 10215).

**Diagnosis.** *Trichomycterus sainthilairei* is distinguished from all other species of *Paracambeva*, except for *T. coelhorum*, *T. humboldti*, *T. pauciradiatus*, *T. piratymbara*, and *T. reinhardti*, by having six pectoral-fin rays (vs. seven). *Trichomycterus sainthilairei* is distinguished from *T. coelhorum* by having more dorsal (17–20 vs. 10–12) and ventral (13–16 vs. 9 or 10) procurrent caudal-fin rays, more vertebrae (37 or 38 vs. 34–36), and more ribs (16 or 17 vs. 12–14); from *T. humboldti* and *T. pauciradiatus* by having five pelvic-fin rays (vs. four); from *T. piratymbara* by having the anal-fin origin at vertical through the posterior half of the dorsal-fin base (vs. anterior half); and from *T. reinhardti* by having fewer dorsal procurrent caudal-fin rays (17–20 vs. 22–25). For a full description and anatomical illustrations, see Costa and Katz (2021).

**Distribution.** *Trichomycterus sainthilairei* is known only from the type locality, in the Córrego do Tamborete, Rio Grande drainage, upper Rio Paraná basin, at about 875 m asl.

**Material examined.** All materials were from Brazil: Estado de Minas Gerais: Município de Capitólio: Córrego Tamborete, Rio Grande drainage, Rio Paraná basin. UFRJ 10215, holotype; UFRJ 9886, six paratypes; UFRJ 9911, six paratypes; UFRJ 9971, five paratypes (C&S); CICC AA 04085, three paratypes; Brazil: Minas Gerais State: Capitólio Municipality: 20°38'53" S 46°09'55" W, at about 875 m asl; A.M. Katz & P.H.N. Bragança, 14 February 2014. MZUSP 87188, 15 paratypes; same locality as holotype; C. Oliveira, 15 April 2005. MNRJ 28660, 33 paratypes; Km 300 of the road MG-050; P.A. Buckup et al., 6 November 2004.

*Trichomycterus (Paracambeva) septemradiatus* Katz, Barbosa & Costa, 2013

Figure 15

*Trichomycterus septemradiatus* Katz, Barbosa & Costa, 2013: [8] (360) (original description; type locality: stream tributary of Cuiabá river, tributary of Grande river [correctly tributary of Rio Sapucaí], Paraná river basin, between villages Conceição da Aparecida and Nova Resende [correctly road Fazenda Cuiabá], Município de Conceição da Aparecida, Estado de Minas Gerais, Brazil, 21°04'24" S 46°12'04" W, at an altitude of 856 m; holotype: UFRJ 8576, 45.4 mm SL).



**Figure 15.** *Trichomycterus (Paracambeva) sainthilairei*. Holotype, UFRJ 10215, Capitólio, 65.4 mm SL: (A) lateral, (B) dorsal, and (C) ventral views.

**Diagnosis.** *Trichomycterus septemradiatus* is distinguished from all other species of *Paracambeva*, except for *T. adautoleitei*, *T. anaisae*, *T. funebris*, *T. ingaiensis*, and *T. luetkeni* by having seven pectoral-fin rays (vs. six in all other species of the *T. reinhardti* group). *Trichomycterus septemradiatus* differs from *T. adautoleitei* by having fewer ventral procurrent caudal-fin rays (10 vs. 13), a longitudinal body stripe with diffuse margins, which is weakly contrasting with the pale yellow ground of the flank (vs. well delimited black stripe, strongly contrasting with the yellow ground of the flank), the absence of round black spots on the dorsum body (vs. presence), and the presence of a longitudinal row of small black spots on the dorsal portion of the flank (vs. absence); from *T. anaisae* and *T. luetkeni* by having fewer dorsal (15 vs. 21–23) and ventral (10 vs. 15–17) procurrent caudal-fin rays; from *T. anaisae* by the absence of two rows of black spots overlapping the longitudinal body stripe (vs. presence); from *T. funebris* by having a shorter latero-posterior process of the autopalatine, with its length being about half of the autopalatine length (vs. about two-thirds), and the anal-fin origin at vertical through the centrum of the 23rd vertebra (vs. 25th or 26th); and from *T. ingaiensis* by having the anal-fin origin at vertical between the base of the fifth dorsal-fin ray (vs. base of the seventh and ninth dorsal-fin rays). For a full description and anatomical illustrations, see Costa and Katz (2021).

**Distribution.** *Trichomycterus septemradiatus* occurs in the Rio Sapucaí subdrainage, Rio Grande drainage, Rio Paraná basin, at altitudes between about 855 and 1040 m asl (Figure 3C).

**Material examined.** All specimens were from Brazil: Estado de Minas Gerais: Rio Grande drainage, Rio Paraná basin. Município de Conceição da Aparecida. UFRJ 8576, holotype, 45.4 mm SL; UFRJ 7278, 11 paratypes; UFRJ 8385, 3 paratypes (C&S); stream tributary to Rio Cuiabá, Rio Sapucaí subdrainage, road Fazenda Cuiabá, 21°04'24'' S 46°12'04'' O, about 855 m asl; J.P.B. Barata, R. Paiva & M.A. Barbosa, 24 November 2006. UFRJ 5088, 1; Córrego Cuiabá, road Fazenda Cuiabá, about 2 km from Conceição da Aparecida, 21°05'22'' S 46°13'43'' W, about 910 m asl; M.A. Barbosa et al., 16 February 2000. UFRJ 9888, 5; UFRJ 9913, 2; same locality as UFRJ 5088; A. M. Katz & P.H. Bragança, 14 February 2014. Município de Carmo do Rio Claro: UFRJ 8283, 6; UFRJ 8373, 4; UFRJ 9689, 2 (C&S); UFRJ 9690, 1 ex (C&S); Ribeirão Santa Quitéria, Cachoeira Pedra Molhada, 21°00'23'' S 46°15'00'' W, about 855 m asl; V.M. Azevedo-Santos, 3 Aug. 2011. UFRJ 12940, Figure 16, 6 ex.; same locality as preceding; A.M. Katz & V.M. Azevedo-Santos, 30 October 2021.



**Figure 16.** *Trichomycterus (Paracambeva) septemradiatus*. UFRJ 12940, Carmo do Rio Claro, 57.8 mm SL: (A) lateral, (B) dorsal, and (C) ventral views.

### 3.3. Key to Identification of *Trichomycterine* Species from MRGD

- 1A. Colour pattern of flank characterized by dark dots over entire flank → 2
- 1B. Colour pattern of flank characterized by longitudinal dark stripe on flank midline → 7
- 2A. Pelvic fin and girdle usually absent, rarely rudimentary → 3
- 2B. Pelvic fin and girdle always well-developed → 5
- 3A. Caudal fin margin aligned with caudal peduncle, forming spatula-like tail; 24 or 25 dorsal and 20 ventral procurent caudal-fin rays → *T. listruroides*
- 3B. Caudal fin margin not aligned with caudal peduncle; 17–20 dorsal and 13–18 ventral procurent caudal-fin rays → 4
- 4A. 17 or 18 ventral procurent caudal-fin rays; 16–19 interopercular odontodes; 21–25 teeth on dentary; minute dark brown dots, equal or smaller than orbital diameter → *T. candidus*
- 4B. 13–16 ventral procurent caudal-fin rays; 21–24 interopercular odontodes; 29–32 teeth on dentary; minute dark brown dots, equal or smaller than orbital diameter → *T. uberabensis*
- 5A. Caudal peduncle expanded dorsally; 29–32 dorsal and 19 or 20 ventral procurent caudal-fin rays → *T. garbei*
- 5B. Caudal peduncle not expanded dorsally; 18–21 dorsal and 13–18 ventral procurent caudal-fin rays → 6
- 6A. Flank dots separated by interspaces that are larger than dots → *T. pirabitira*
- 6B. Flank dots separated by interspaces that are smaller than dots → *T. saturatus*
- 7A. Seven pectoral-fin rays → 8
- 7B. Six pectoral-fin rays → 9
- 8A. Pectoral-fin filament about 40% of pectoral-fin length excluding filament; dorsum with black spots; dorsal part of the flank without longitudinal series of dark dots; longitudinal midline stripe of flank well-delimited, black and highly contrasting with yellow ground; 13 ventral procurent caudal-fin rays → *T. adautoleitei*
- 8B. Pectoral-fin filament about 20% or less of pectoral-fin length excluding filament; dorsum without black spots; dorsal part of the flank with longitudinal series of dark dots; longitudinal midline stripe of flank diffuse, dark grey and weakly contrasting with pale yellow ground; 10 dorsal procurent caudal-fin rays → *T. septemradiatus*
- 9A. 10–12 dorsal and 9 or 10 ventral procurent caudal-fin rays → *T. coelhorum*
- 9B. 17–20 dorsal and 13–16 ventral procurent caudal-fin rays → *T. saintthilairei*

## 4. Discussion

### 4.1. Phylogenetic Relationships of *Trichomycterines* from the MRGD

The phylogenetic analysis indicates that the six species of *Cryptocambeva* endemic to the MRGD belong to two major intrageneric clades (Figure 1). *Trichomycterus garbei* is highly supported as a member of a clade containing two other species, which do not occur in the Rio Grande drainage: *Trichomycterus araxa* Costa, Mattos, Sampaio, Giongo, Almeida & Katz, 2022, from the Rio Paranaíba drainage, upper Rio Paraná basin [22], and *Trichomycterus macrotrichopterus* Barbosa & Costa, 2010, from the upper Rio São Francisco basin [43]. This clade corresponds to the Canastra clade in Costa et al. [22], but no unique apomorphic morphological character state shared by these three species was found here. According to Costa et al. [22], sister-group relationships between *T. araxa* and *T. macrotrichopterus* are morphologically supported by both species sharing the presence of a long pectoral-fin filament, with its length being about 40–60% of the pectoral-fin length in specimens about 50 mm SL or larger. However, this apomorphic condition is not present in *T. garbei*, suggesting that *T. araxa* and *T. macrotrichopterus* are more closely related to each other than to *T. garbei*, but the resolution within this clade was low in the present molecular analysis (Figure 1).

The other five species of *Cryptocambeva* from the MRGD are basal members of a clade that also includes species endemic to the Rio Paraíba do Sul basin and adjacent smaller coastal basins: *Trichomycterus claudiae* Barbosa & Costa, 2010, *Trichomycterus mirissumba*

Costa, 1992, *T. potschi* Barbosa & Costa, 2003, and *T. vermiculatus* (Eigenmann, 1917). This clade corresponds to the southern Mantiqueira-Mar clade in Costa et al. [22].

A group comprising *T. candidus* and *T. uberabensis* is highly supported in the molecular analysis, but *T. listruoides*, which was not included in this analysis, is clearly a member of the clade, the *T. candidus* complex. In all three species, the pelvic fin and girdle are absent. Among the over 130 specimens belonging to this species complex examined in the present study, only two specimens have a single rudimentary pelvic fin, with three and four minute rays, respectively. In addition, these species also share a small anterior projection of the anterior margin of the dorsal process of the interopercle, close to the area attached to the ligament connecting the interopercle and lower jaw (Figure 6B,F), which is not present in other species of *Cryptocambeva*; a posterior expansion of the metapterygoid (Figure 6B,F) that is present only in the distantly related *Trichomycterus mimonha* Costa, 1992, among the species of *Cryptocambeva*; and a relatively short premaxilla that is shorter than the maxilla (Figure 5B,D) and bears fewer teeth than in other species of *Cryptocambeva* (19–28 vs. 36–70), except for *Trichomycterus giarettai* Barbosa & Katz, 2016 (27–30 premaxillary teeth), a species from the Rio Paraíba drainage [44] not included in the molecular analysis. *Trichomycterus giarettai*, a species with well-developed pelvic fin and girdle, is probably the sister group of the *T. candidus* complex because all the species share low counts of jaw teeth and odontodes. *Trichomycterus candidus* and *T. listruoides* are probably sister taxa. They share the presence of a deep concavity on the anterior margin of the interopercle and a metapterygoid that is much longer than deep (Figure 6B), and few teeth on the dentary (21–25), which are conditions that do not occur in other members of *Cryptocambeva* and closely related taxa, thus being considered apomorphies.

Despite *T. pirabitira* and *T. saturatus* being morphologically very similar, the analysis indicates that these two species are not sister taxa. *Trichomycterus saturatus* is strongly supported as a member of the clade including just species from the Rio Paraíba do Sul basin and smaller coastal basins. No unambiguously derived morphological character state was found to corroborate this clade, but the included taxa are the largest species of *Cryptocambeva*, reaching at least about 120 mm SL, which may be interpreted as an evolutionarily relevant factor supporting monophyly. *Trichomycterus pirabitira* is supported as sister to a clade including *T. saturatus*, a species from the Rio Paraíba do Sul basin and adjacent coastal areas, and a species of the *T. candidus* complex. However, no morphological character was found to corroborate this clade.

The four species of *Paracambeva* appear in a weakly supported clade containing all species endemic of the upper Rio Paraná basin (Figure 1), corresponding to the Serra da Mantiqueira clade in Costa and Katz (2021). In this tree topology, *T. coelhorum* appears as sister to all other species of this clade; *T. adautoleitei* is strongly supported as sister to *T. septemradiatus*, thus forming a two-species clade endemic to the MRGD, and *T. saintilhairi* is strongly supported as sister to a clade including *Trichomycterus funebris* Katz & Costa, 2021 and *Trichomycterus ingaiensis* Katz & Costa, 2021, two species endemic to the upper sections of the Rio Grande drainage [1]. No morphological character was found to support these relationships.

#### 4.2. Distribution Patterns of *Trichomycterines* in the MRGD

Our field studies detected the occurrence of one, two, or three trichomycterine species in each collecting site. In cases where we found two or three sympatric species, they invariably comprised one species of *Cryptocambeva* of the *T. candidus* complex (i.e., small pelvic-less species), one species of *Cryptocambeva* belonging to another lineage (i.e., large species with well-developed pelvic fin and girdle), and one species of *Paracambeva*. In addition, sympatric species often exhibit similar distribution patterns (compare Figure 3A–C), indicating the existence of different areas of endemism within the MRGD.

The Rio Uberaba, a tributary of the right bank of the Rio Grande at the western-most part of the MRGD, is inhabited by *T. coelhorum* of *Paracambeva* (Figure 3C) and *T. uberabensis* of the *T. candidus* complex (Figure 3B), which then characterize an area of endemism

(i.e., area of distribution of two or more species), the Uberaba area. *Trichomycterus garbei* was found alone in a single locality in the Rio Canoas subdrainage, a tributary of the left margin of the Rio Grande (Figure 3A); thus, its occurrence was not informative to delimitate an area of endemism.

*Trichomycterus pirabityra* is a species from the MRGD with the widest distribution (Figure 3A). It occurs in the south-eastern part of the MRGD, between the Rio São João and Rio Sapucaí subdrainages that are at the left margin of the Rio Grande (Figure 3A). A similar distribution pattern was found for *T. candidus*, with this species encompassing the distribution of two populations identified here as *Trichomycterus* cf. *candidus* (Figure 3B), thus configuring an area of endemism, the São João-Sapucaí area. This area is also inhabited by the clade comprising *T. adautoleitei* and *T. septemradiatus*, with the former species endemic to an area east of the Rio Sapucaí, and the latter species occurring in areas west of that river (Figure 3C).

Finally, three species, *T. listruoides*, *T. saintilhareii*, and *T. saturatus*, were only found in a single small area in the Córrego Tamborete, a small tributary of the right margin of the Rio Grande, thus being considered as a distinct area of endemism, the Tamborete area.

#### 4.3. Areas of Endemism and Conservation of Trichomycterines from the MRGD

Areas of endemism play an important role in delimiting priority areas for conservation, especially in regions that combine a high rate of endemism with a constant increase in factors that threaten the survival of species, as in the MRGD. The species studied here are known from small watercourses of the Rio Grande drainage, which are under strong pressure from anthropogenic activities, such as small dams for water supply, irrigation and hydroelectric power generation [3], removal of vegetation for watering cattle and mining activities, and contamination by urban and rural effluents (V.M. Azevedo-Santos, personal observation). Furthermore, small fish species have been threatened by the introduction of trout in the Rio Grande basin [45], which is a voracious predator. Even leisure activities, such as bathers visiting waterfalls in the region, can negatively impact ichthyofauna, especially through the introduction of plastic and chemical wastes, such as sunscreen and suntan lotions (V.M. Azevedo-Santos, personal observation). This scenario suggests that the MRGD trichomycterines are at least endangered, but more detailed field surveys are necessary to evaluate the present conservation state of the local fauna of small fish species. Despite the existence of protected areas in the headwater zones belonging to the Rio Grande drainage [46], all species recorded here for the MRGD occur outside these areas.

Among the areas of endemism delimited here, the Tamborete area has particular relevance for the conservation of the MRGD species. This is a small area, about 50 km<sup>2</sup>, confined between the Serra da Canastra and the Rio Grande at the Furnas dam that, in addition to the three endemic trichomycterine species, shelters two endemic species of armoured catfishes, (Loricariidae), *Pareiorhina pelicicei* Azevedo-Santos & Roxo, 2015, and *Neoplecostomus canastra* Roxo, Silva, Zawadzki & Oliveira, 2017 [1,9,10], thereby adding value to its importance for conservation. Despite the Tamborete area being close to the Serra da Canastra National Park, it is outside the area protected by Brazilian legislation. Therefore, the Tamborete area must be considered as a priority area for the conservation of the MRGD biodiversity.

The São João-Sapucaí area is also of some relevance because, in addition to harbouring a total of four trichomycterine species (see above), the same stream where *T. adautoleitei* occurs is the type locality of another species of catfish, *Heptapterus carmelitanorum* Azevedo-Santos, Deprá, Aguilera, Faustino-Fuster & Katz, 2022 (Heptapteridae), which is known only from small populations in this area [11]. Additional field studies in the Rio Uberaba area, where we currently have records of two endemic trichomycterine species known from only one locality (see above), are needed to determine the extent of the distribution area of these species. Similarly, the subdrainage of the Rio Canoas basin, an area of occurrence of *T. garbei* and populations of *Aeglea franca* Schmitt, 1942 (Bueno et al., 2007), a crustacean listed as critically endangered in the official list of the Brazilian Government (MMA) [47], needs further field studies to determine the possible occurrence of other endemic species.

## 5. Conclusions

This study is an example that despite the global importance of endemic mountain biota for delimitation of biodiversity hotspots, some members of the fauna and flora of tropical mountainous regions are still insufficiently known, even in areas close to large urban centres such as the MRGD. Our reports firstly reveal a diversified segment of the mountain ichthyofauna from the MRGD, including descriptions of six new species, highlighting the importance of integrating osteological characters and molecular phylogenies to support species diagnoses and placement. Our data additionally show that efforts should be made to delineate small mountain areas with multiple endemic species as units for conservation strategic proposals.

**Author Contributions:** Conceptualization, W.J.E.M.C.; data obtaining, W.J.E.M.C., J.L.O.M., V.M.A.-S. and A.M.K.; formal analysis, W.J.E.M.C. and J.L.O.M.; investigation and data curation, W.J.E.M.C., J.L.O.M. and A.M.K.; writing—original draft preparation, W.J.E.M.C.; writing—final version, W.J.E.M.C., J.L.O.M., V.M.A.-S. and A.M.K.; visualization, W.J.E.M.C., J.L.O.M. and A.M.K.; supervision, W.J.E.M.C.; project administration, W.J.E.M.C.; funding acquisition, W.J.E.M.C. and A.M.K. All authors have read and agreed to the published version of the manuscript.

**Funding:** This study was supported by the Conselho Nacional de Desenvolvimento Científico e Tecnológico (CNPq; grant 304755/2020-6 to WJEMC), and the Fundação Carlos Chagas Filho de Amparo à Pesquisa do Estado do Rio de Janeiro (FAPERJ; grant E-26/201.213/2021 to WJEMC, E-26/202.327/2018 to JLOM; and E-26/202.005/2020 to AMK). This study was also supported by the CAPES (Finance Code 001) through the Programa de Pós-Graduação em: Biodiversidade e Biologia Evolutiva/UFRJ and Genética/UFRJ.

**Institutional Review Board Statement:** The animal study protocol was approved by the Ethics Committee for Animal Use of Federal University of Rio de Janeiro (protocol code: 065/18, approved on August 2018).

**Data Availability Statement:** DNA sequences used in this study are deposited in GenBank.

**Acknowledgments:** We are grateful to P. N. Coelho and family for logistic support during field studies, and F. Tinti, R. Ferrazi, and G. Correia-Silva for help during field collections. The manuscript benefitted from the criticisms and suggestions provided by the three anonymous reviewers.

**Conflicts of Interest:** The authors declare no conflict of interest. The funders had no role in the design of the study; in the collection, analyses, or interpretation of data; in the writing of the manuscript; or in the decision to publish the results.

## Appendix A

**Table A1.** Terminal taxa for molecular phylogeny and respective GenBank accession numbers.

	COX1	CYTB	RAG2
<i>Diplomystes nahuelbutaensis</i>	AP012011.1	MN640588.1	DQ492317.1
<i>Nematogenys inermis</i>	EU359428	-	KY858182
<i>Callichthys callichthys</i>	MZ051783.1	KP960058.1	DQ492324.1
<i>Trichogenes longipinnis</i>	MK123682	MK123704	MF431117
<i>Microcambeva ribeirae</i>	MN385807.1	OK334290.1	MN385832.1
<i>Ituglanis boitata</i>	MK123684	MK123706	MK123758
<i>Trichomycterus areolatus</i>	AP012026.1	AP012026.1	KY858188
<i>Scleronema minutum</i>	MK123685	KY858031	KY858184
<i>Cambeva barbosa</i>	MK123689.1	OQ110808	MN385820.1
<i>Trichomycterus itatiayae</i>	MW671552	MW679291	OL779233
<i>Trichomycterus anaisae</i>	MT941782	MT941820.1	OQ660182

**Table A1.** Cont.

	COX1	CYTB	RAG2
<i>Trichomycterus luetkeni</i>	MT941793	MT941831.1	KY858214
<i>Trichomycterus reinhardti</i>	MK123698	MK123727	MF431119
<i>Trichomycterus coelhorum</i>	OQ648152	OQ660192	OQ660183
<i>Trichomycterus adautoleitei</i>	OQ648153	OQ660193	-
<i>Trichomycterus septemradiatus</i>	MT941818.1	MT941854.1	MW196781
<i>Trichomycterus piratymbara</i>	KY857970	KY858040	KY858194
<i>Trichomycterus humboldti</i>	MT941787	MT941824	OQ660184
<i>Trichomycterus pauciradiatus</i>	MT941796	MT941833.1	MW196782
<i>Trichomycterus sainthilairei</i>	MT941816.1	MT941853.1	OQ660185
<i>Trichomycterus funebris</i>	MT941785	MT941823	KY858194
<i>Trichomycterus ingaiensis</i>	MT941790	MT941829	OQ660186
<i>Trichomycterus nigricans</i>	MN813005	MK123723	MK123765
<i>Trichomycterus albinotatus</i>	MN813007	MK123716	MN812990
<i>Trichomycterus vitalbrazili</i>	MT435137	MK748279.1	MT446428
<i>Trichomycterus mimonha</i>	MW196749)	MW196758	MW196783
<i>Trichomycterus pirabitira</i>	OQ660199	OQ660194	OM540758.1
<i>Trichomycterus candidus</i>	OQ357890	OQ355714	OQ400961
<i>Trichomycterus uberabensis</i>	OQ648154	OQ660195	OQ660187
<i>Trichomycterus saturatus</i>	OQ660200	OQ660196	OQ660188
<i>Trichomycterus mirissumba</i>	MW196752	MW196761	MW196786
<i>Trichomycterus potschi</i>	-	MW196763	MW196789
<i>Trichomycterus vermiculatus</i>	OQ648155	OQ660197	OQ660189
<i>Trichomycterus claudiae</i>	MW196754	MW196764.1	MW196790
<i>Trichomycterus novalimensis</i>	MW196755.1	MW196765.1	MW196791
<i>Trichomycterus brasiliensis</i>	MK123691	MK123717	MK123763
<i>Trichomycterus rubiginosus</i>	MK123699	MK123728	MK123767
<i>Trichomycterus araxa</i>	OQ648156	OM250023	OM250025
<i>Trichomycterus macrotrichopterus</i>	MW196753	MW196762.1	MW196787
<i>Trichomycterus garbei</i>	-	OQ660198	OQ660190
<i>Trichomycterus fuliginosus</i>	MW196750	MW196759	MW196784
<i>Trichomycterus brunoii</i>	MW19675	MW196760	MW196785
<i>Trichomycterus argos</i>	OQ357887	OQ355711	OQ660191

**Appendix B****Table A2.** Best-fitting partition schemes and evolutive models.

Partition	Base Pairs	Evolutive Model
tRNA(Tyr)	57	K80 + I
COX1 1st	232	TRN + G
COX1 2nd	232	TRN + I + G
COX1 3rd	231	TVM + I
CYTB 1st	343	HKY + I + G
CYTB 2nd	343	GTR + I + G
CYTB 3rd	343	TVMEF + I + G
RAG2 1st	273	TVMEF + I + G
RAG2 2nd	273	TVM + G
RAG2 3rd	272	TVMEF + G

## References

1. Costa, W.J.E.M.; Katz, A.M. Integrative taxonomy supports high species diversity of south-eastern Brazilian mountain catfishes of the *T. reinhardti* group (Siluriformes: Trichomycteridae). *Syst. Biodivers.* **2021**, *19*, 601–621. [CrossRef]
2. CEMIG (Companhia Energética de Minas Gerais). *Guia Ilustrado de Peixes da Bacia do Rio Grande*; CETEC: Belo Horizonte, Brazil, 2000.
3. Belei, F.; Sampaio, W.M.S. Ictiofauna do rio Lourenço Velho, afluente do Rio Grande: Pequena diversidade, grande importância para a conservação de uma espécie ameaçada. *Evol. Conserv. Biodivers.* **2012**, *3*, 14–27. [CrossRef]
4. Paiva, M.P.; Andrade-Tubino, M.F.; Godoy, M.P. *As Represas e os Peixes Nativos do rio Grande*; Interciência: Rio de Janeiro, Brazil, 2002.
5. Azevedo-Santos, V.M.; Britski, H.A.; Oliveira, C.; Benine, R.C. Ichthyofauna of streams of the Rio Sapucaí basin, upper Rio Paraná system, Minas Gerais, Brazil. *Biota Neotrop.* **2019**, *19*, e20180617. [CrossRef]
6. Bockmann, F.A.; Ribeiro, A.C. Description of a new suckermouth armored catfish of the genus *Pareiorhina* (Siluriformes: Loricariidae), from southeastern Brazil. *Ichthyol. Explor. Freshw.* **2003**, *14*, 447–458.
7. Barbosa, M.A.; Azevedo-Santos, V.M. A new species of the catfish genus *Trichomycterus* (Teleostei: Siluriformes: Trichomycteridae) from the rio Paraná basin, southeastern Brazil. *Vertebr. Zool.* **2012**, *62*, 357–362. [CrossRef]
8. Katz, A.M.; Barbosa, M.A.; Costa, W.J.E.M. Two new species of the catfish genus *Trichomycterus* from the Paraná river basin, southeastern Brazil (Teleostei: Trichomycteridae). *Ichthyol. Explor. Freshw.* **2013**, *23*, 359–366.
9. Azevedo-Santos, V.M.; Roxo, F.F. A new species of the genus *Pareiorhina* (Teleostei: Siluriformes: Loricariidae) from the upper rio Paraná basin, southeastern Brazil. *Zootaxa* **2015**, *3937*, 377–385. [CrossRef]
10. Roxo, F.F.; Silva, G.S.C.; Zawadzki, C.H.; Oliveira, C. *Neoplecostomus canastra*, a new catfish (Teleostei: Siluriformes) species from upper Rio Paraná basin. *Zootaxa* **2017**, *4294*, 226–240. [CrossRef]
11. Depra, G.C.; Aguilera, G.; Faustino-Fuster, D.R.; Katz, A.M.; Azevedo-Santos, V.M. Redefinition of *Heptapterus* (Heptapteridae) and description of *Heptapterus carmelitanorum*, a new species from the upper Paraná River basin in Brazil. *Zoosystematics Evol.* **2022**, *98*, 327–343. [CrossRef]
12. Costa, W.J.E.M.; Mattos, J.L.O.; Katz, A.M. Two new catfish species from central Brazil comprising a new clade supported by molecular phylogeny and comparative osteology (Siluriformes: Trichomycteridae). *Zool. Anz.* **2021**, *293*, 124–137. [CrossRef]
13. Castellanos-Morales, C.A.; Marino-Zamudio, L.L.; Guerrero, L.; Maldonado-Ocampo, J.A. Peces del Departamento de Santander, Colombia. *Rev. Acad. Colomb. Cienc.* **2011**, *35*, 189–212.
14. Hayes, M.M.; Paz, H.J.; Stout, C.C.; Werneke, D.C.; Armbruster, J.W. A hotspot atop: Rivers of the Guyana Highlands hold high diversity of endemic pencil catfish (Teleostei: Ostariophysi: Siluriformes). *Biol. J. Linn. Soc.* **2020**, *129*, 862–874. [CrossRef]
15. Costa, W.J.E.M.; Feltrin, C.R.M.; Katz, A.M. Field inventory reveals high diversity of new species of mountain catfishes, genus *Cambeva* (Siluriformes: Trichomycteridae), in south-eastern Serra Geral, southern Brazil. *Zoosystema* **2021**, *43*, 659–690. [CrossRef]
16. Costa, W.J.E.M.; Mattos, J.L.; Vilardo, P.J.; Amorim, P.F.; Katz, A.M. Perils of underestimating species diversity: Revisiting systematics of *Psammocambeva* catfishes (Siluriformes: Trichomycteridae) from the Rio Paraíba do Sul Basin, south-eastern Brazil. *Taxonomy* **2022**, *2*, 491–523. [CrossRef]
17. Costa, W.J.E.M.; Feltrin, C.R.M.; Mattos, J.L.O.; Dalcin, R.H.; Abilhoa, V.; Katz, A.M. Morpho-Molecular Discordance? Re-Approaching systematics of *Cambeva* (Siluriformes: Trichomycteridae) from the Guaratuba-Babitonga-Itapocu Area, southern Brazil. *Fishes* **2023**, *8*, 63. [CrossRef]
18. Reis, R.B.d.; Ferrer, J.; Graça, W.J.d. A new species of *Cambeva* (Siluriformes, Trichomycteridae) from the Rio Iguçu basin, Paraná state, Brazil and redescription of *Cambeva stawiarski* (Miranda Ribeiro 1968). *J. Fish Biol.* **2021**, *96*, 350–363. [CrossRef] [PubMed]
19. Miranda Ribeiro, P. Notas para o estudo dos Pygidiidae brasileiros (Pisces, Pygidiidae, Pygidiinae). *Bol. Mus. Nac. Rio. Jan.* **1949**, *88*, 1–3.
20. Leary, S.; Underwood, W.; Anthony, R.; Cartner, S.; Corey, D.; Grandin, T.; Greenacre, C.; Gwaltney-Brant, S.; McCrackin, M.; Meyer, R.; et al. AVMA Guidelines for the Euthanasia of Animals: 2020 Edition. 2020. Available online: <http://www.avma.org/sites/default/files/2020-02/Guidelines-on-Euthanasia-2020.pdf> (accessed on 3 December 2022).
21. Taylor, W.R.; Van Dyke, G.C. Revised procedures for staining and clearing small fishes and other vertebrates for bone and cartilage study. *Cybium* **1985**, *9*, 107–119.
22. Costa, W.J.E.M.; Mattos, J.L.O.; Sampaio, W.M.S.; Giongo, P.; Almeida, F.B.d.; Katz, A.M. Phylogenetic relationships of a new catfish of the genus *Trichomycterus* (Siluriformes, Trichomycteridae) from the Brazilian Cerrado, and the role of Cenozoic events in the diversification of mountain catfishes. *Zoosyst. Evol.* **2022**, *98*, 151–164. [CrossRef]
23. Costa, W.J.E.M. Description de huit nouvelles espèces du genre *Trichomycterus* (Siluriformes: Trichomycteridae), du Brésil oriental. *Rev. Française D'aquariologie Herpetol.* **1992**, *18*, 101–110.
24. Costa, W.J.E.M.; Katz, A.M.; Mattos, J.L.O.; Amorim, P.F.; Mesquita, B.O.; Vilardo, P.J.; Barbosa, M.A. Historical review and redescription of three poorly known species of the catfish genus *Trichomycterus* from south-eastern Brazil (Siluriformes: Trichomycteridae). *J. Nat. Hist.* **2020**, *53*, 2905–2928. [CrossRef]
25. Bockmann, F.A.; Sazima, I. *Trichomycterus maracaya*, a new catfish from the upper rio Paraná, southeastern Brazil (Siluriformes: Trichomycteridae), with notes on the *T. brasiliensis* species-complex. *Neotrop. Ichthyol.* **2004**, *2*, 61–74. [CrossRef]
26. Costa, W.J.E.M. Comparative osteology, phylogeny and classification of the eastern South American catfish genus *Trichomycterus* (Siluriformes: Trichomycteridae). *Taxonomy* **2021**, *1*, 160–191. [CrossRef]
27. Arratia, G.; Huaquin, L. Morphology of the lateral line system and of the skin of diplomystic and certain primitive loricarioid catfishes and systematic and ecological considerations. *Bonn Zool. Monogr.* **1995**, *36*, 1–110.

28. Unmack, P.J.; Bennin, A.P.; Habi, E.M.; Victoriano, P.F.; Johnson, J.B. Impact of ocean barriers, topography, and glaciation on the phylogeography of the catfish *Trichomycterus areolatus* (Teleostei: Trichomycteridae) in Chile. *Biol. J. Linn. Soc.* **2009**, *97*, 876–892. [[CrossRef](#)]
29. Villa-Verde, L.; Lazzarotto, H.; Lima, S.Q.M. A new glanapterygine catfish of the genus *Listrura* (Siluriformes: Trichomycteridae) from southeastern Brazil, corroborated by morphological and molecular data. *Neotrop. Ichthyol.* **2012**, *10*, 527–538. [[CrossRef](#)]
30. Ward, R.D.; Zemlak, T.S.; Innes, B.H.; Last, P.R.; Hebert, P.D. DNA barcoding Australia's fish species. *Philos. Trans. R. Soc. Lond. B Biol. Sci.* **2005**, *360*, 1847–1857. [[CrossRef](#)]
31. Costa, W.J.E.M.; Henschel, E.; Katz, A.M. Multigene phylogeny reveals convergent evolution in small interstitial catfishes from the Amazon and Atlantic forests (Siluriformes: Trichomycteridae). *Zool. Scr.* **2020**, *49*, 159–173. [[CrossRef](#)]
32. Tamura, K.; Stecher, G.; Kumar, S. MEGA11: Molecular Evolutionary Genetics Analysis Version 11. *Mol. Biol. Evol.* **2021**, *38*, 3022–3027. [[CrossRef](#)]
33. Chenna, R.; Sugawara, H.; Koike, T.; Lopez, R.; Gibson, T.J.; Higgins, D.G.; Thompson, J.D. Multiple sequence alignment with the Clustal series of programs. *Nucleic Acids Res.* **2003**, *31*, 3497–3500. [[CrossRef](#)]
34. Lanfear, R.; Frandsen, P.B.; Wright, A.M.; Senfeld, T.; Calcott, B. PartitionFinder 2: New methods for selecting partitioned models of evolution for molecular and morphological phylogenetic analyses. *Mol. Biol. Evol.* **2017**, *34*, 772–773. [[CrossRef](#)]
35. Suchard, M.A.; Lemey, P.; Baele, G.; Ayres, D.L.; Drummond, A.J.; Rambaut, A. Bayesian phylogenetic and phylodynamic data integration using BEAST 1.10. *Virus Evol.* **2018**, *4*, 1–5. [[CrossRef](#)]
36. Gernhard, T. The conditioned reconstruction process. *J. Theor. Biol.* **2008**, *253*, 769–778. [[CrossRef](#)]
37. Rambaut, A.; Drummond, A.J.; Xie, D.; Baele, G.; Suchard, M.A. Posterior summarisation in Bayesian phylogenetics using Tracer 1.7. *Syst. Biol.* **2018**, *67*, 901–904. [[CrossRef](#)] [[PubMed](#)]
38. Minh, B.Q.; Schmidt, H.A.; Chernomor, O.; Schrempf, D.; Woodhams, M.D.; von Haeseler, A.; Lanfear, R. IQ-TREE 2: New models and efficient methods for phylogenetic inference in the genomic era. *Mol. Biol. Evol.* **2020**, *37*, 1530–1534. [[CrossRef](#)] [[PubMed](#)]
39. Hoang, D.T.; Chernomor, O.; von Haeseler, A.; Minh, B.Q.; Vinh, L.S. UFBoot2: Improving the ultrafast bootstrap approximation. *Mol. Biol. Evol.* **2018**, *35*, 518–522. [[CrossRef](#)] [[PubMed](#)]
40. Felsenstein, J. Confidence limits on phylogenies: An approach using the bootstrap. *Evolution* **1985**, *39*, 783–791. [[CrossRef](#)]
41. Barbosa, M.A.; Costa, W.J.E.M. Validade, relações filogenéticas e redescricao de *Eremophilus candidus* Ribeiro, 1949 (Teleostei, Siluriformes, Trichomycteridae). *Arq. Mus. Nac. Rio. Jan.* **2003**, *61*, 179–188.
42. Azevedo-Santos, V.M.; Coelho, P.N.; Brambilla, E.M.; Lima, F.P.; Nobile, A.B.; Britton, J.R. Length-weight relationships of four fish species from the upper Paraná River basin, Southeastern Brazil. *J. Appl. Ichthyol.* **2018**, *34*, 237–239. [[CrossRef](#)]
43. Barbosa, M.A.; Costa, W.J.E.M. Seven new species of the catfish genus *Trichomycterus* (Teleostei: Siluriformes: Trichomycteridae) from Southeastern Brazil and redescription of *T. brasiliensis*. *Ichthyol. Explor. Freshw.* **2010**, *21*, 97–122.
44. Barbosa, M.A.; Katz, A.M. A new species of the catfish genus *Trichomycterus* (Teleostei: Siluriformes: Trichomycteridae) from the Paranaíba basin, Central Brazil. *Vertebr. Zool.* **2016**, *66*, 261–265. [[CrossRef](#)]
45. Magalhães, A.L.B.; Andrade, R.F.; Ratton, T.F.; Brito, M.F.G. Ocorrência da truta arco-íris *Oncorhynchus mykiss* (Walbaum, 1792) (Pisces: Salmonidae) no alto rio Aiuruóca e tributários, bacia do rio Grande, Minas Gerais, Brasil. *Bol. Mus. Biol. Mello Leitão* **2002**, *14*, 35–42.
46. Azevedo-Santos, V.M.; Frederico, R.G.; Fagundes, C.K.; Pompeu, P.S.; Pelicice, F.M.; Padial, A.A.; Nogueira, M.G.; Fearnside, P.M.; Lima, L.B.; Daga, V.S.; et al. Protected areas: A focus on Brazilian freshwater biodiversity. *Divers. Distrib.* **2019**, *25*, 442–448. [[CrossRef](#)]
47. MMA (Ministério do Meio Ambiente). Portaria GM/MMA N° 300, de 13 de Dezembro de 2022. Available online: <https://www.in.gov.br/en/web/dou/-/portaria-gm/mma-n-300-de-13-de-dezembro-de-2022-450425464> (accessed on 18 March 2023).

**Disclaimer/Publisher's Note:** The statements, opinions and data contained in all publications are solely those of the individual author(s) and contributor(s) and not of MDPI and/or the editor(s). MDPI and/or the editor(s) disclaim responsibility for any injury to people or property resulting from any ideas, methods, instructions or products referred to in the content.